Cover page--Final Progress Report-TBI individual grant

John Pintar
Dept. Neuroscience and Cell Biology
Robert Wood Johnson Medical School
683 Hoes Lane
Piscataway, NJ 08854

Title: The role of IGF binding proteins in response to brain injury

Grant Number: 09-32-12 BIR-E2

Period covered: 6/1/09-6/30/12

Submitted: 12/28/12

1. Original Aims of Project

The insulin-like growth factor (IGF) system functions as a major regulator of cell survival and proliferation. This system consists not only of two ligands (IGF-1 and IGF-II) and at least three receptors, but also several extracellular binding proteins (IGFBPs) that modulate IGF actions. IGF-1 signaling through the Akt pathway is known to promote cell survival in multiple CNS neuronal and glial cell types, and several clinical trials using IGF-I as a therapeutic agent for a variety of neurodegenerative conditions have already been undertaken. These trials have not yet led to effective therapeutic outcomes, probably because there are multiple regulators of IGF action, still poorly understood, that may have significantly influenced the outcomes of these studies. Evidence from both in situ hybridization and gene array studies have indicated that several IGFBPs are up-regulated at multiple locations in models of brain injury. In particular, IGFBPs 2, 3, 4 and 5 are up-regulated in the area of lesion following both hypoxia-ischemia and penetrating wound models while, more recently, we have shown significant up-regulation of IGFBP-2 at the injury site in mice following a controlled cortical impact (CCI) injury. Gene targeting in the mouse has been used to produce novel experimental models that have led to major advances in understanding the role of specific genes in both normal and abnormal disease processes. We have produced and characterized at multiple levels several gene-targeted KO models of IGFBPs (including KOs of IGFBP 2,3,4,5, and 6). We now propose to investigate whether these IGFBP mutant strains (with initial emphasis on the IGFBP-2 KO) show significant alterations from the wild-type patterns in the extent of neural and glial apoptosis as well as proliferative responses of cells near the CCI wound site and in the SVZ. We propose two specific aims:

1. **We find in preliminary experiments that IGFBP-2 is significantly up-regulated in the mouse for at least a week following moderate CCI** (1 mm deformation, 4m/sec, duration 150msec), while preliminary data indicate that other IGFBPs may also exhibit altered expression in this model. We will first document this upregulation and begin to assess the functional significance of this IGFBP-2 up-regulation on several cellular processes near the injury site. We will assess whether expression of other IGFBPs is altered in the absence of IGFBP-2, whether the invasion of microglia/macrophages (potential sources of IGF-I) is altered at specific early time points following injury, and also assess whether apoptosis of neurons, oligodendrocytes, or oligodendroctye precursors is altered at early time points following lesion by using activated caspase 3 detection in conjunction with cell-type specific markers. These experiments will allow us to determine whether cellular sources of IGF-1 are altered in IGFBP-2 (or other) KO mice following CCI, whether the absence of IGFBP-2 (or other IGFBP) enhances or limits apoptosis of neurons and other cell types near the injury.

2. **We find that IGFBP-2 is expressed at relatively high levels in CNS-derived neurospheres.** We will complement analysis of injury site responses in IGFBP KO mice in Aim 1 by determining whether the number and proliferative responses of neural progenitor cells in the SVZ (a potential source of restorative cells) are altered in adult IGFBP KO mice either basally or following CCI TBI, again focussing initially on the IGFBP-2 KO. If alterations in proliferation are detected, we will evaluate changes in specific SVZ subpopulations using a recently developed nestin-nuclear-cyan fluorescent protein (CFP) transgenic mouse.

Together these experiments will test the hypothesis that the absence of members of the IGFBP gene family alters the cellular response(s) to CCI TBI. These studies will thus provide the first genetic investigation of IGFBP function following this clinically relevant model of TBI and therefore will be critical in evaluating the role of the IGF system in protection, repair and restoration following traumatic injury.

2. Project Successes

We made substantial progress toward the overall goal of our project to investigate the role of IGF binding proteins following traumatic brain injury. We were successful in introducing the compression injury model for TBI since it is currently thought to be a far better model to provide information related to the goals of the NJ Commission on TBI. We were successful in showing that the same IGFBPs upregulated following the puncture wound model were also be up-regulated in wild-type mice following compression injury (see below). We then began to determine the consequences of IGFBP-2 mutation using the general overall strategy we had proposed for previously analyzing effects from the puncture wound model with a major focus on proliferative alterations following mutation. As a significant extension of the proposed study, we examined IGFBP-3 KO for alterations in proliferation, with this extension based on the altered cortical structure of IGFBP-3 KO mice that we hypothesized might also indicate altered responses following TBI.

All TBI experiments were performed using the e-Controlled Cortical Impactor (CCI) manufactured by Custom-Design in Virginia. TBI was produced using this impactor with the injury depth of deformation 1 mm, velocity at 4 m/sec and duration of 150 msec. Ten-twelve mice could be put through this procedure in one day, so that we have been able to examine time-course outcomes following injury of a single cohort of mice. We found that the cavity formed by the wound is clear at day 3 and maintained at day 7 and is similar to a recent analysis of mice following a lateral compression injury of similar severity (J. Neurotrauma 23:1241).

Once the model was established, we began to determine whether there are any changes in IGFBP expression following CCI. Following lateral CCI using the conditions above, individual sets of mice were maintained for 0, 1, 3, and 7 days. Brains were then isolated, fresh-frozen, and processed for in situ hybridization with several 35S-labelled IGFBP probes. Sections from two-four fresh-frozen brains were examined at each age. One specific IGFBP, IGFBP-2, was found to be upregulated in the parenchyma adjacent to the injury site, with the results for the expression pattern similar at each time point following CCI. Low IGFBP-2 expression is normally seen at the X-ray level only in the meninges and choroids plexus. Even one day following CCI, however, low levels of IGFBP-2 expression were detected near the lesion site, while prominent up-regulation was apparent in nearby meninges. The upregulation of IGFBP-2 was also clear and more dramatic at both day 3 and 7 following CCI. The higher level of IGFBP-2 ipsilateral expression at day 3 compared to the contralateral site is readily apparent with expression relatively evenly distributed through the parenchyma adjacent to the lesion site (arrows, Fig. 1A), as well as in nearby meninges. At day 7, IGFBP-2 has increased from day 3, with the pattern more focused around the lesion site (Fig. 1B). These results were presented in abstract form at the International IGF Congress (Qin et al., 2010; abstract appended). Interestingly, the overall pattern of IGFBP-2 expression is generally similar between the models and similar to that of reactive gliosis described for the mouse following lateral CCI (Saatman et al., 2006). The above data clearly demonstrated that IGBP-2 was up-regulated following CCI TBI.

To determine the possible functional significance of this up-regulation, three cohorts of IGFBP-2 KO mice and wild-type controls have now been bred to adulthood, undergone CCI, been maintained for both 3- and 7-post CCI, and then fixed for histological examination. Broad histological analysis of these mice several aspects of the proposed analysis have been completed. The most significant observation is that proliferation in the IGFBP-2 mutants (as assayed by BrdU incorporation following injection 4 hrs before sacrifice; n=3) is up-regulated at both ages compared to WT both near the injury site (Fig. 2) as well as in the SVZ (Fig. 3) where p=0.06 for n=3 in the 3-

day cohort compared to WT control. The SVZ result is consistent with the hypothesis that IGFBP-2 normally inhibits proliferative effects of IGF-1 following TBI and that IGFBP-2 absence will likely impact the IGF signaling that is enhanced following TBI. Staining with GFAP indicated no significant change in activated astrocytes as well as the lack of overlap between BuDR labeling and GFAP labeling (Fig. 4), neuN (neurons), and Iba-1 (microglia)(not shown). Interestingly, it has become clear that other IGFBP KO mutants also show phenotypes consistent with the possibility that IGFBPs more generally inhibit IGF proliferative activity. This important aspect of IGFBP function was not evident on mixed genetic backgrounds but has become clear on the C57Bl/6 background (Gleason et al., 2010).

We have also begun to screen all IGFBP mutants for phenotypes that might impact interpretation of responses to TBI. This phenotyping was initiated following the completion of backcrossing to C57Bl6/J inbred strain. To begin this anatomic study of all IGFBP mutants, we (in collaboration with Roko Rasin) fixed and stained brain sections (focusing on cortex) from WT and IGFBP mutant mice using several antibodies that recognize immunologic markers with restricted expression in discrete cortical layers. We have found several changes in the cortical organization of IGFBP KO brains that are presented in Table 1. Most dramatically, we have found that the IGFBP-3 KO mouse appears to have a dramatic alteration in organization of several upper cortical layers. Our first indication of this phenomenon was that staining for the specific nuclear transcription factor SATB2, which marks cells in cortical layers 2-4, was dramatically reduced compared to WT and all other IGFBP mutants (see Table 1, with n=1-3 brains examined for each strain). Importantly, we have also observed changes in IGFBP-2 KO as well (Table 1), which we will need to consider as we continue analysis and interpretation of results of this line following CCI. We extended histological study of the IGFBP-3 KO to determine whether this alteration in transcription factor expression might also reflect functional markers for cortical neurons in this region. We examined several markers of axonal and dendritic arborization and, again, we have seen quite significant differences between the IGFBP-3 KO and WT using SMI32 and MAP2 to map dendrite organization in specific cortical layers. For example, SMI32 staining is very much reduced and essentially absent in layers 2-4 but not layer 5 of IGFBP-3 KO but not WT mice (Fig. 5) with a similar pattern seen for MAP2. This reduction of staining, though dramatic, has not allowed us to assess directly whether structure/formation of the apical dendrites is impaired, although neural cell number revealed by DAPI staining is unchanged. Thus we are currently extending these studies to examine neuron processes in these cortical regions using Golgi impregnation. This approach should allow us to determine whether structural changes in dendrites characterize IGFBP-3 KO mice, with possible changes in IGFBP-2 KO mice also under study.

Based on the above changes in IGFBP-3 cortical structure, we began to determine whether absence of IGFP-3 might impact responses to TBI. We focused our initial studies on proliferation in IGFBP-3 KO brains and combined study of IGFBP-3 with additional study of IGFBP-2. As shown in Fig. 6, there is an increase in proliferation near the injury site in both IGFBP-2 and IGFBP-3 mutants, raising the question of whether this increase could be even greater in a double KO.

Finally, we continued to investigate isolated neurospheres from early postnatal mice that we found to express high levels of IGFBP2 as well as lower levels of other IGFBPs. We used an alternate method to quantitate the qPCR that documented IGFBP-2 expression (Fig. 7), which was combined with substantial amount of data on the role IGF ligand expression in neurosphere proliferation from the Levison lab that has now been published. Given the increased proliferation in the SVZ of IGFBP-2 KO mice, culturing neurospheres from IGFBP-2 KO mice to determine whether the

proliferation/differentiation characteristics change compared to WT is better justified. Since these assays are already established and can be combined with several assays of stemness developed by the Levison lab, this approach will be best way to determine whether the role of IGFBP-2 in these cells is to promote or inhibit ongoing proliferation and /or differentiation.

3. Project challenges. There were no major limitations though the ability to produce identical lesions in groups of mice was perhaps more challenging that we imagined. Thus we had fewer mice with similar lesions than we had expected but nonetheless were able to make significant progress.

4. Implications. The finding that IGFBP-2 alters proliferation following TBI suggests that IGF ligands that lack IGFBP binding sites may be useful therapeutically. As study of IGFBP-2 and IGFBP-3 mutants following CCI TBI continues, it is important to realize that these studies will begin to determine definitely whether up-regulation of a specific IGFBP will tend to limit protective effects of IGF (as in the mammary gland model and consistent with the data on SVZ proliferation), or alternatively whether any specific IGFBP may help stabilize IGF in the wound area and thus ultimately enhance IGF action. This alternate possibility has been suggested by analysis of the growth alteration in IGFBP-4 mice, where absence of this IGFBP prevents optimal action of IGF during prenatal development (Ning et al., 2008). Interestingly, the basic pattern of IGFBP-2 expression in parenchyma near the wound site is conserved between puncture wound and CCI models, perhaps indicating equivalent function. In fact. preliminary data indicate that proliferation further from the injury site tends to be lower than WT in both the IGFBP-2 and IGFBP-3 mutant mice at both 3- and 7-days.

5. Plans to continue work. We have submitted continuation grants to NJCTBI to extend aspects of this work, though first submission was not funded. We have also submitted an NIH grant that will soon be reviewed that proposes to extend IGFBP-3 data presented above, as well as a letter of intent to the Simons Foundation. There is clear justification as well for examining IGFBP mutants in terms of effects on neurosphere differentiation since these cells may have therapeutic benefit and it is thus critical to understand how the role of IGF-II may be modulated by the IGFBPs expressed during self- renewal and differentiation of these cells, so we anticipate proposing such experiemnts in future applications.

6. Abstracts, publications and presentations:

Abstracts:

Qin, M., Jiang, Y., Peng, B., Cominski, T.P. Levison, S., Pintar, J.E.   Up-regulation of IGFBP-2 following a Controlled Cortical Impact Injury, International GH/IGF meeting, New York, Nov. 2010.

Presentations:

Pintar, J.E. Role of IGFBP-3 in brain development, Gordon Research Conf. March, 2011.

Publications:

Ziegler AN, Schneider JS, Qin M, Tyler WA, Pintar JE, Fraidenraich D, Wood TL, Levison SW (2012). IGF-II promotes stemness of neural restricted precursors Stem Cells Jun;30(6):1265-76.
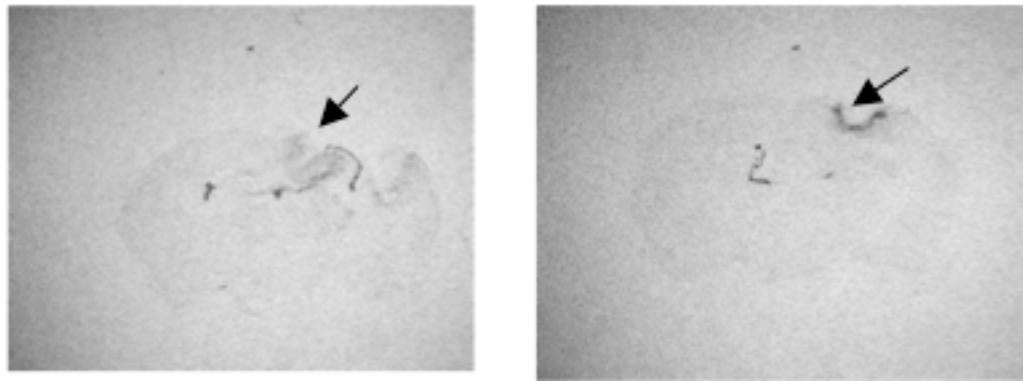
7. Financial report-sent by UMDNJ

Fig. 1. IGFBP-2 is dramatically up-regulated following CCI TBI.
Note increased expression on ipsilateral side at day 3 (left panel)
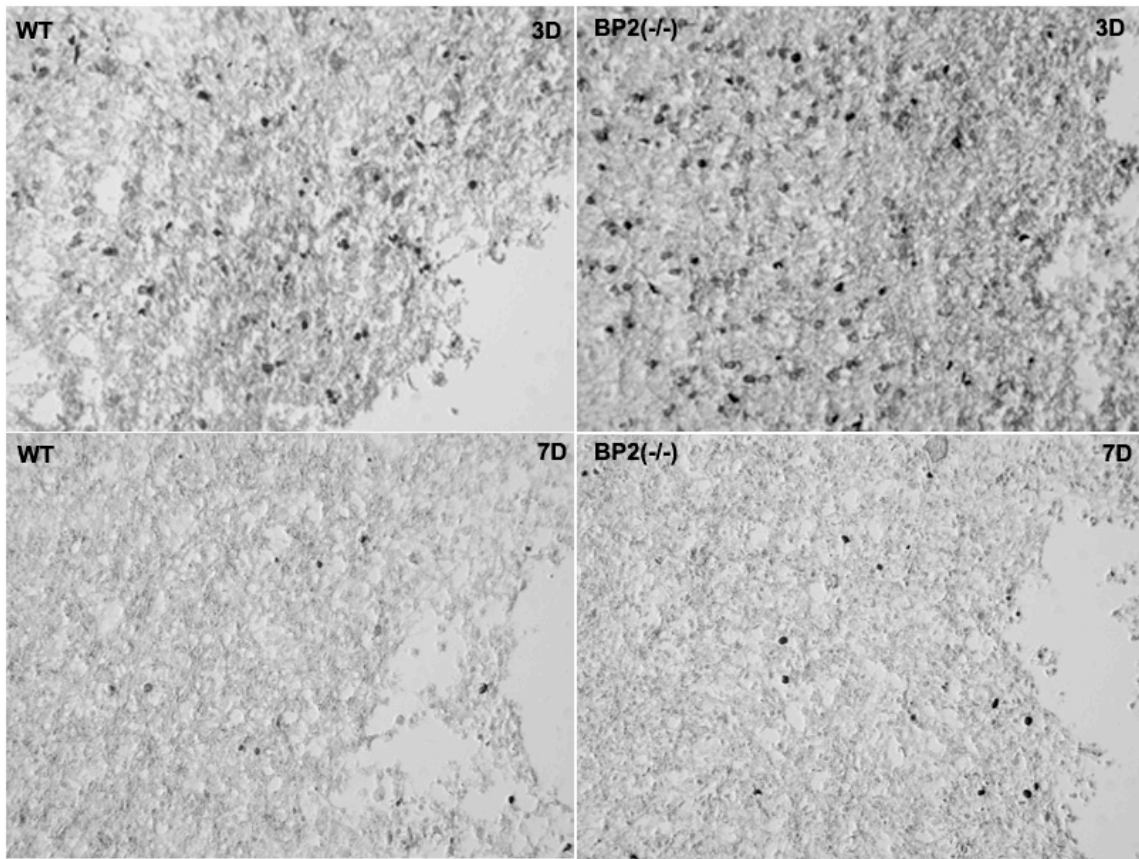and continuing high expression at day 7 (right panel)

Fig. 2. BrdU labeling of the cortical region adjacent to the injury sites at 3-day (upper panels) and 7-day (lower panel) following CCI. Greater labelling is apparent in IGFBP-2 KO.

Fig. 3. Representative micrographs of subventricular BrdU labelling in WT and IGFBP-2 KO mice 3- and 7-days following CCI (mice sacrificed 4 hr after BdrU).
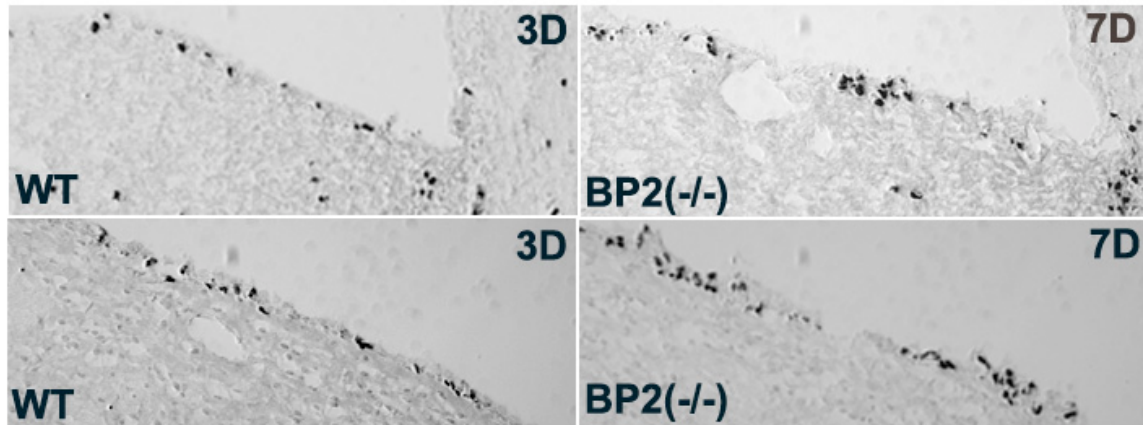
Quantitation of SVZ BdrU labelled cells in WT and IGFBP-2 KO mice. In all cases, BrdU labelling highest in IGFBP-2 and most extensive 7-day following injury. For day 3, $p < 0.05$ IGFBP-2 injured side vs. WT non-injured; $p = 0.06$ WT injured vs. IGFBP-2 injured (n=3); for day 7, counting of additional mice in progress (IGFBP-2 n=2; WT n=1).
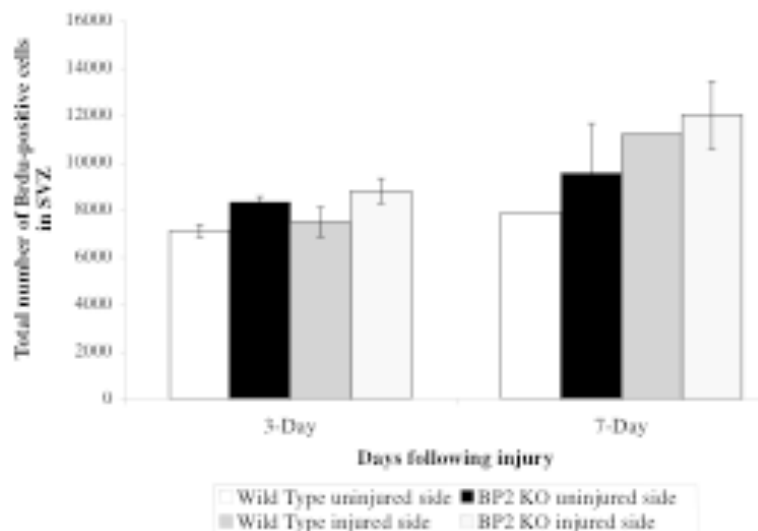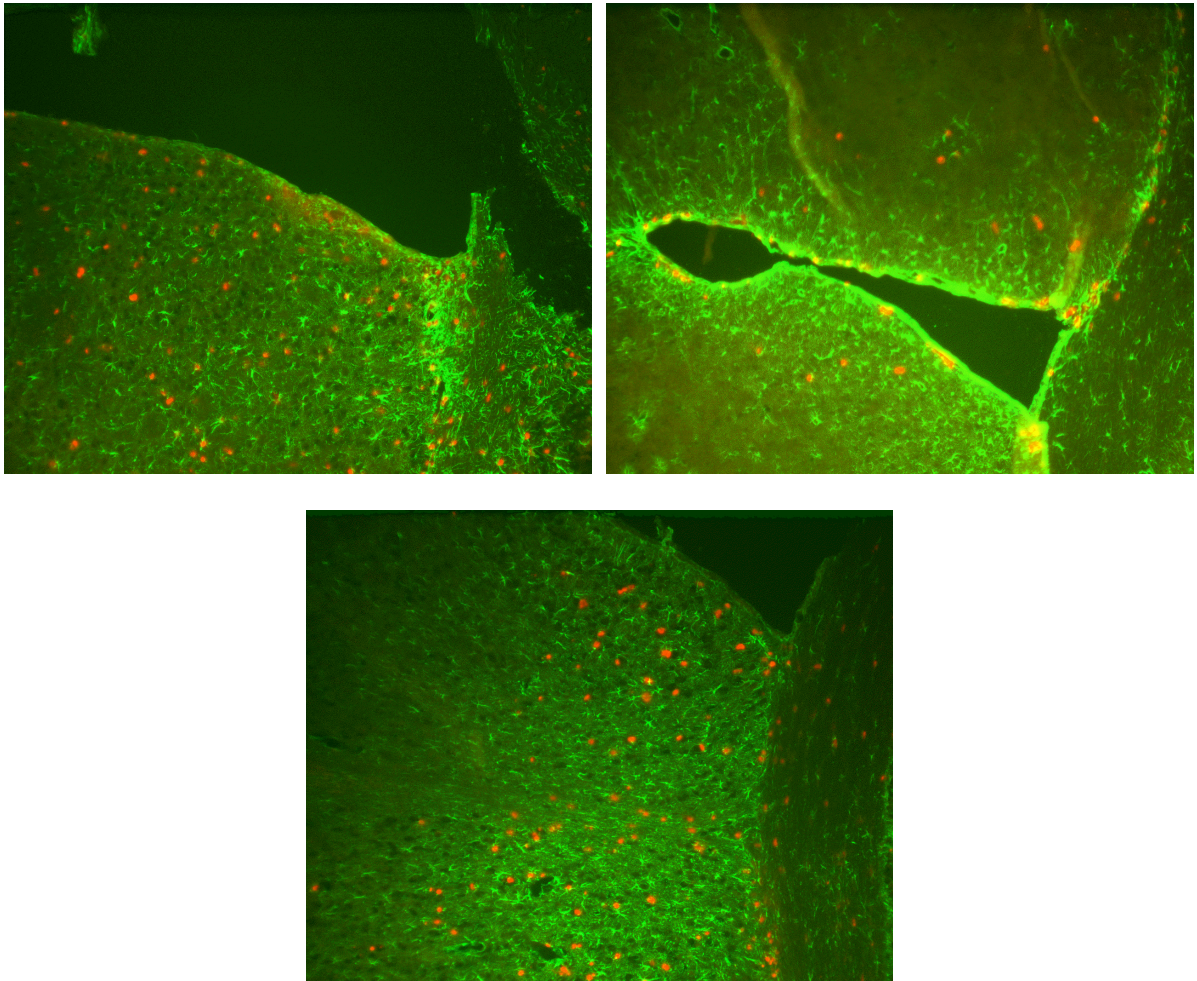
Fig. 4. Dual immunostaining of BuDR and GFAP in WT and IGFBP-2 KO mice 3 days following CCI. The dramatic increase in BuDR (visualized in red) seen near the surface in Fig. 3 is maintained near the 3rd ventricle. The number of GFAP positive cells (green) appears similar in both genotypes following TBI.
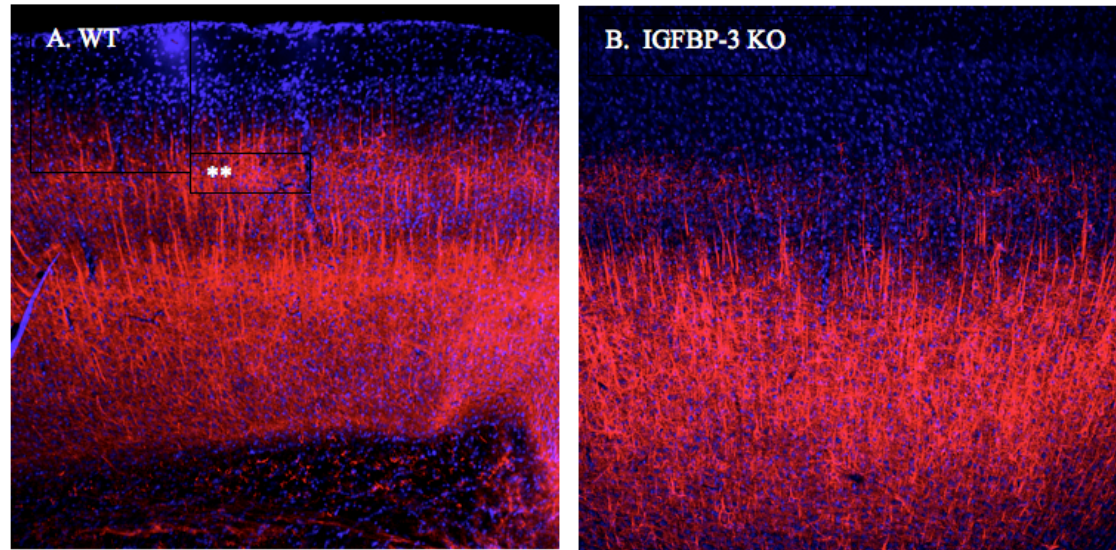
Fig. 5. SMP32 staining of cortex from WT (A) and IGFBP-3 KO (B). The dramatic decrease in staining of SMP32 (red) in the upper cortical layers (asterisks) of the IGFBP-3 KO mouse compared to WT is evident. IGFBP-2 KO mice, though showing a slight alteration in SATB2 staining (Table 1), has not shown any difference in SMP-32 staining as yet (not shown).

Fig. 6: BrdU labeling increased near injury site at day 7 post-CCI in both IGFP-2 and IGFBP-3 KO mice

BrdU labelling following TBI - 3 days Recovery
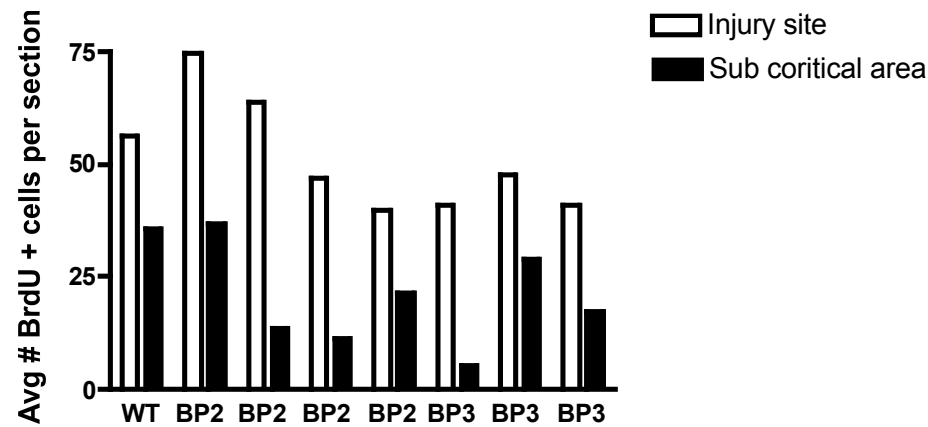
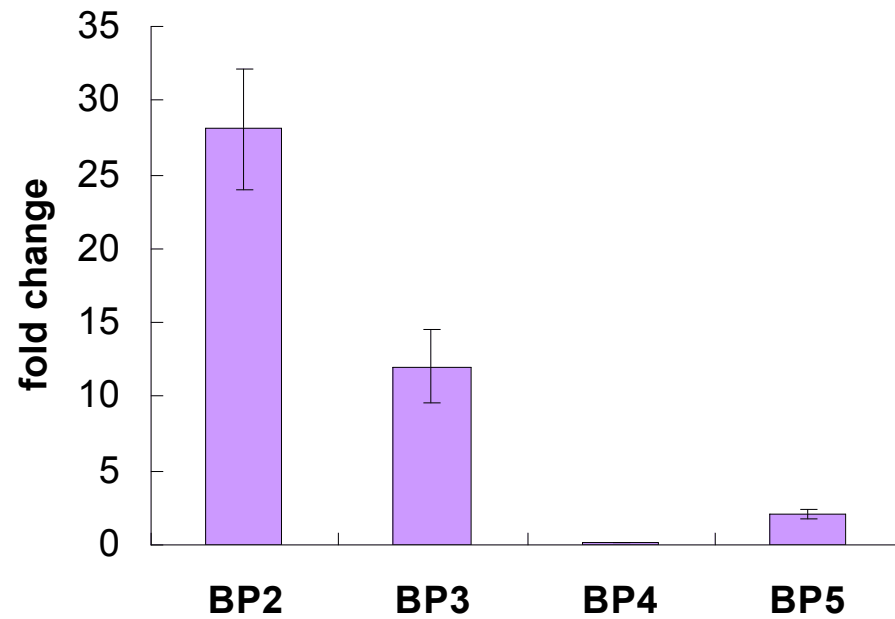**BrdU labelling following TBI - 7 days Recovery**
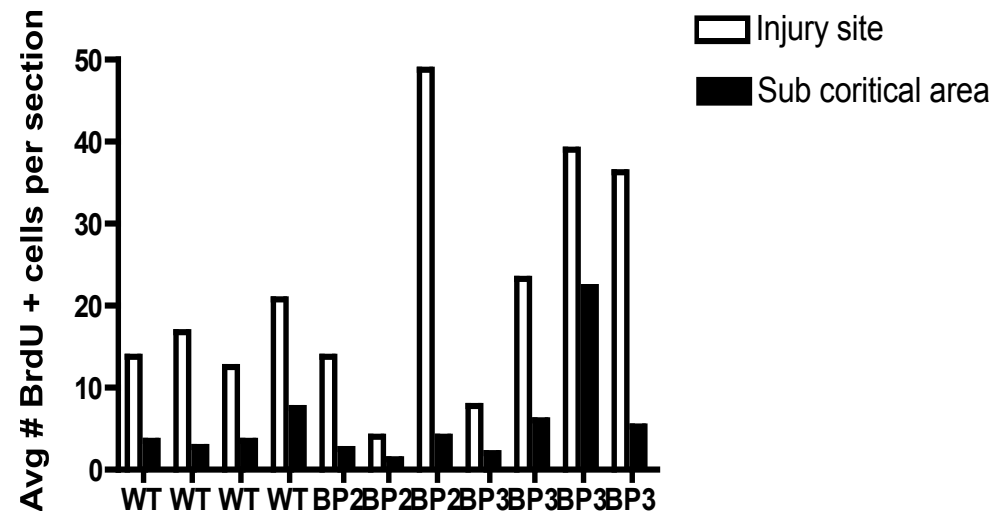
Fig. 7. Neurospheres were cultured from the SVZ of P5 mice and mRNA was extracted and reverse transcribed to cDNA. Real-time qPCR was run with GAPDH as reference gene and Stratagene's Universal Mouse Reference cDNA as control. The qPCR with each primer set was run three times, each time in triplicate. The results are presented in bar graph form and show that IGFBP-2, -3, -5 are up-regulated 28-, 12-, and 2-fold respectively compared to the reference standard. In contrast, IGFBP-4 is down-regulated 8-fold; no signals were obtained with IGFBP-5 and IGFBP-6.

Table 1. Distribution of cortical specific markers in C57Bl6/J +/+ and IGFBP 1-6 KO mice that have been backcrossed onto the C57Bl6/J background. Staining for the layer-specific transcription factor SATB2 is absent in IGFBP-3 KO mice and shows altered expression in IGFBP-2 KO mice.

	SATB2	FoxP2	Bcl11b	CDP
WT Adult (-/-)	+	Layer 5 +	Layer 5 +	+
		Layer 6 +	Layer 6 +	
BP3 (-/-) (n=4)	-	Layer 5 -	Layer 5 +	+
		Layer 6 +	Layer 6 +/-	
BP6 (-/-) (n=2)	+/-	Layer 5 -	Layer 5 +	+
		Layer 6 +	Layer 6 +/-	
BP5 (-/-)	+/-	Layer 5 +/-	Layer 5 +	+
		Layer 6 -	Layer 6 +/-	
BP1 #1 (-/-)	+	layer 5 +		
		layer 6 +		
BP1 #2 (-/-)	+/-	layer 5 +		
		layer 6 +		
BP1 #3 (-/-)	+	layer 5 +/-		
		layer 6 +		
BP2 #1 (-/-)	+	layer 5 +/-		
		layer 6 +		
BP2 #2 (-/-)	+	layer 5 -		
		layer 6 +		
BP2 #3 (-/-)	+	layer 5 +		
		layer 6 +		

For BP2 --> SATB2 is positive in upper layers and ectopic in lower layers; sensory specific

Up-regulation of IGFBP-2 following a controlled cortical impact injury. Mei Qin, Yuhui Jiang, Bonnie Peng, Tara Cominsk, Steven Levison, and John Pintar, RWJMS and NJMS, UMDNJ, Piscataway, NJ

We have previously documented up-regulation of several of the IGFBPs via puncture wound (Berry, Logan, Pintar) and sought to determine whether the more physiologically relevant compression model for TBI (controlled cortical impact) would lead to alterations in IGFBP expression following this type of injury. We found thar one specific IGFBP, IGFBP-2, was reproducibly up-regulated in the parenchyma adjacent to the injury site, with the results for the expression pattern similar at several time points following CCI. Low IGFBP-2 expression is un-injured mice is normally seen at the X-ray level only in the meninges and choroids plexus. However, even only one day following CCI, low levels of IGFBP-2 expression are detected near the lesion site while prominent up-regulation is apparent in the nearby meninges. The up-regulation of IGFBP-2 remains clear and more dramatic at both day 3 and 7 following CCI. The higher levels of expression at day 3 are readily apparent with expression relatively evenly distributed through the brain parenchyma adjacent to the lesion site. By day 7 following lesion, expression is focused around the lesion site though expression appears to be increased from that of day 4. These results clearly demonstrated that IGFBP-2 expression is upregulated near the impact site for at least 7 days and suggest that perhaps the increased expression is maintained over an even longer period. This long-lasting expression is in contrast to our earlier work with IGFBP expression in the puncture wound model, where IGFBP-2 was up-regulated 2-4 days post-lesion, but had resolved to normal levels by day 7 following injury. These results indicate that IGFBP-2 near the injury site in a TBI model may modulate IGF signaling, which has also recently been shown to be regulated by CCI. Supported by New Jersey Commission on Traumatic Brain Injury.

While IGF-1 has been shown to impact nervous system development, no evidence to date has implicated any of the IGFBPs (expressed in the different patterns in the developing CNS) in this process in either an IGF-dependent or IGF-independent role. We have now initiated neuroanatomical phenotyping of all IGFBP KO mice following completion of backcrossing (F10) to the C57Bl6/J strain. To begin anatomic study of the cerebral cortex of IGFBP mutant mice, we stained brain sections from WT and IGFBP mutant mice with multiple antibodies that recognize immunologic markers having restricted expression in discrete cortical layers. We have found several changes in the neocortical organization of IGFBP KO brains. Most dramatically, we have found that IGFBP-3 KO mice have a dramatic alteration in organization of upper layers of sensorimotor neocortices. The first indication of this phenomenon came from preliminary studies using antisera to the nuclear transcription factor SATB2, which marks cells in cortical layers 2-4; staining was dramatically reduced in IGFBP3 KO mice compared to WT. We extended histological study of IGFBP-3 KO to determine whether this alteration in transcription factor expression might also reflect alterations in functional markers of neocortical circuitry organization. Therefore, we examined several markers of axonal and dendritic arborization. Again, significant differences between IGFBP-3 KO and WT mice in dendritic polarity were observed using the dendrite markers SMI32 and MAP2. Thus SMI32 staining is very much reduced and essentially absent in layers 2-4 but not layer 5 of IGFBP-3 KO but not WT mice, with a similar pattern seen for MAP2. To confirm this dendritic phenotype, we performed in utero electorporations into a single hemisphere of developing sensorimotor neocortices at e15.5, when upper layer neurons are born, using a vector expressing GFP. Electroporated embryos were left to survive until postnatal day 14. We found disrupted polarity of neocortical projection neurons of the upper layers at this age as well as decreased axonal projections via the corpus callosum into contralateral hemisphere. This approach confirmed that the dendritic polarity and arborization of upper layer cortical neurons is altered in IGFBP-3 KO mice. Together these results indicate that the fetal cortical expression of IGFBP-3 contributes to the phenotypic differentiation of a subset of sensorimotor neocortical neurons. Supported by the New Jersey Commission on Traumatic Brain Injury.

Stem Cells®

Tissue-Specific Stem Cells

IGF-II Promotes Stemness of Neural Restricted Precursors

Amber N. Ziegler,[a] Joel S. Schneider,[b] Mei Qin,[c] William A. Tyler,[a] John E. Pintar,[c] Diego Fraidenraich,[b] Teresa L. Wood,[a] Steven W. Levison[a]

[a]Department of Neurology and Neuroscience and [b]Department of Cell Biology and Molecular Medicine, New Jersey Medical School, University of Medicine and Dentistry of New Jersey, Newark, New Jersey, USA; [c]Department of Neuroscience and Cell Biology, University of Medicine and Dentistry of New Jersey, Piscataway, New Jersey, USA

Abstract

Insulin-like growth factor (IGF)-I and IGF-II regulate brain development and growth through the IGF type 1 receptor (IGF-1R). Less appreciated is that IGF-II, but not IGF-I, activates a splice variant of the insulin receptor (IR) known as IR-A. We hypothesized that IGF-II exerts distinct effects from IGF-I on neural stem/progenitor cells (NSPs) via its interaction with IR-A. Immunofluorescence revealed high IGF-II in the medial region of the subventricular zone (SVZ) comprising the neural stem cell niche, with IGF-II mRNA predominant in the adjacent choroid plexus. The IGF-1R and the IR isoforms were differentially expressed with IR-A predominant in the medial SVZ, whereas the IGF-1R was more abundant laterally. Similarly, IR-A was more highly expressed by NSPs, whereas the IGF-1R was more highly expressed by lineage restricted cells. In vitro, IGF-II was
more potent in promoting NSP expansion than either IGF-I or standard growth medium. Limiting dilution and differentiation assays revealed that IGF-II was superior to IGF-I in promoting stemness. In vivo, NSPs propagated in IGF-II migrated to and took up residence in periventricular niches while IGF-I-treated NSPs predominantly colonized white matter. Knockdown of IR or IGF-1R using shRNAs supported the conclusion that the IGF-1R promotes progenitor proliferation, whereas the IR is important for self-renewal. Q-PCR revealed that IGF-II increased Oct4, Sox1, and FABP7 mRNA levels in NSPs. Our data support the conclusion that IGF-II promotes the self-renewal of neural stem/progenitors via the IR. By contrast, IGF-1R functions as a mitogenic receptor to increase precursor abundance. Stem Cells 2012;30:1265–1276

Disclosure of potential conflicts of interest is found at the end of this article.

Introduction

Stem cells throughout the body are found within specialized niches. Like other stem cell niches, the neural stem cell (NSC) niche is a complex microenvironment and is elegantly organized to favor specific cell-cell interactions as well as access to the cerebral microvasculature, extracellular matrix components, meninges, and cerebral spinal fluid (CSF). Whereas the lineage of NSCs within the subventricular zone (SVZ) as well as the generation and migration of neural stem/progenitor cell (NSP) progeny has been an area of intense focus, the niche microenvironment has only recently been studied in detail. NSCs reside in the center of a pinwheel structure surrounded by ependymal cells that produce Noggin to inhibit the actions of bone morphogenetic proteins to maintain NSC properties [1, 2]. The NSCs also extend a process that contacts microvessels within the SVZ, enabling them to respond to factors in the circulation. The NSC niche is rich in

fibroblast growth factor 2 and laminin both of which are localized to structures called fractones [3]. These factors have been shown to promote NSC self-renewal via $\alpha6\beta1$ integrin and FGFR1 [4, 5]. Other cell-cell interactions within the niche influence NSCs; for example, adherens junctions and the Par complex promote Notch signaling in the ventricular zone (VZ) that helps to maintain the NSCs in a primitive, radial glial state, by promoting symmetric division [6, 7]. Retinoic acid is yet another factor that is supplied in part by the niche. The meninges, a major source of retinoic acid, have recently been shown to be important for corticogenesis from VZ NSCs [8].

Another source of growth factors and cytokines that promote NSC maintenance is the choroid plexus, which produces CSF. NSCs extend a process that contacts the CSF [9]. CNTF/LIF, SLIT, and TGF-β are produced by the choroid plexus and secreted into CSF to affect NSCs. A gradient of CNTF/LIF is necessary to maintain VZ cells during the development of the ventral forebrain [10] and SLIT, like CNTF/LIF, is found along a gradient in the SVZ. The specialized

organization of the ciliated ependymal cells not only controls the flow of the CSF but also establishes the gradient of SLIT and possibly other factors that are found within the CSF that may affect niche cells [11].

The insulin-like growth factors (IGF) are abundant in the CSF. Interestingly, circulating IGF-I declines approximately 14% per decade, and recently it was shown that IGF-II levels within the CSF also decline with age [12–14]. Despite some evidence that insulin and the IGFs affect embryonic stem cells (ESCs), NSCs, and mesenchymal stem cells, the IGFs and insulin have not received the attention they are due [15–17]. The IGF system is highly complex consisting of two ligands and multiple signaling receptors with varying binding capabilities and downstream effects. There are two IGF ligands, IGF-I and IGF-II, along with four receptors, IGF-1R, insulin receptor (IR), hybrid receptor (a heterodimer of IGF-1R and IR), and IGF-2R/mannose-6-phosphate receptor [18–20]. IGF-I binds with high affinity to both the IGF-1R and the hybrid receptor. IGF-II binds with high affinity to IGF-1R, IR-A, and the hybrid receptor. Furthermore, the IGF system is modulated by six IGF binding proteins (IGFBPs) that may enhance or abrogate IGF actions [19]. The goal of the studies reported here was to test the hypothesis that IGF system activation is essential for NSP growth and that individual receptors and ligands distinctly regulate the growth, self-renewal, and maintenance of NSPs.

MATERIALS AND METHODS

Neurosphere Propagation, Quantification, and Differentiation

The periventricular region of C57Blk/6 pups (P4-5) was enzymatically dissociated for 15 minutes at 37°C using 0.25% trypsin/EDTA Invitrogen (Carlsbad, CA, www.invitrogen.com) and 100 units Papain Sigma (St. Louis, MO, www.sigma.com) in MEM-HEPES with 250 μg/ml of DNase I (Sigma) and 3 mM MgSO$_4$. The tissue was triturated in 0.01% trypsin inhibitor (Sigma) in Pro-N media [21]. The cells were plated into wells at 1×10^5 cells per milliliter in media supplemented with 20 ng/ml recombinant human epidermal growth factor (EGF) PeproTech (Rocky Hill, NJ, www.peprotech.com). Cultures were fed every 2 days by replacing half of the media with an equal volume of fresh media. Neurospheres were collected after 8 and 9 days in vitro (DIV) by centrifugation at 200g for 5 minutes. They were dissociated for 5 minutes at 37°C in Acutase Millipore (Billerica, MA, www.millipore.com) and plated into 12-well plates at 5×10^4 cells per milliliter in Pro-N media either with 4.4 nM or with 4.4 μM insulin (Sigma) supplemented with 20 ng/ml EGF and either with human recombinant IGF-I (Millipore) or with mouse recombinant IGF-II R&D Systems Inc. (Minneapolis, MN, www.rndsystems.com). IMC-A12 was provided by ImClone Systems, a wholly owned subsidiary of Eli Lilly and Co. IR function-blocking antibody (MA1-16812 ThermoFisher (Wilmington, DE, www.thermofisher.com)) was used at a final concentration of 10 nM in medium containing 1 μM insulin.

Neurospheres were quantified as described previously [21]. Neurosphere volume was determined from phase-contrast images using a Zeiss Axiovision Observer.Z1 Carl Zeiss, Inc. (Thornwood, NY, www.zeiss.com) microscope under ×10 or ×40 magnification. Axiovision software was used to measure neurosphere diameters of a minimum of 50 randomly selected neurospheres per condition.

Spheres were collected and resuspended in 2% normal calf serum in Pro-N media at a density of ∼100–200 spheres per milliliter and plated onto 1% poly(D-lysine) and 10 mg/ml laminin-coated chamberslides. After sphere attachment media were replaced with 250 μl of 0.5% normal calf serum in Pro-N and differentiated for 5–7 days. Cells were stained using O4 supernatant (1:3), TuJ1 (Covance, Princeton, NJ, www.covance.com; 1:500), glial fibrillary acidic protein (GFAP) (DAKO; 1:500), and GAM IgM 549, 488, and GAR AMCA (Jackson ImmunoResearch West Grove, PA, www.jacksonimmunno.com; 1:200). Images were captured using a SenSys cooled-coupled device camera interfaced with IP Lab scientific imaging software (Scanalytics, Fairfax, VA, www.spectraservices.com) on an Olympus AX-70 microscope.

Limiting Dilution Analysis

Secondary spheres were cultured in the assay conditions and then passaged into 96-well plates at 7,500, 5,000, 2,500, 1,000, 500, and 250 cells per centimeter square in 200 μl Pro-N with 4.4 μM insulin and EGF at 20 ng/ml. After 7 DIV, the natural log of the fraction of negative wells was plotted against the plating density, using the equation $p = 1 - e^{mD}$ (p is probability, m is slope, and D is density). The intercept of the linear regression at $y = -1$ corresponds to 37%, which is the frequency of cells capable of forming a neurosphere according to a Poisson distribution [22].

Transplantation Studies

Secondary neurospheres generated from a tomato red expressing mouse (The Jackson Laboratory Bar Harbor, ME www.jax.org strain 007576) were maintained for 6 DIV, dissociated into a single cell suspension, and resuspended in culture medium to a concentration of 20,000 cells per 0.5 μl. The cells were transplanted into P21 C57/Blk6 mice at +1.1 mm, 0.6 mm lateral to midline, and 2 mm below skull. Measurements are from bregma. Cells were allowed to differentiate in situ for 30 days, after which the mice were perfused, sectioned sagittally at 40 μm on a cryostat, stained, and imaged on a Nikon A1R laser scanning confocal microscope. A total of six hemispheres from three animals were analyzed for each group. All experiments on animals were carried out in accordance with institutional guidelines. Animal protocols were submitted and reviewed by the NJMS IACUC committee. The present authors further attest that all efforts were made to minimize the number of animals used and their suffering.

Isolation of Total RNA

The entire SVZ, cortex, and choroid plexus were dissected from various ages of c57Blk/6 mice and processed for RNA as previously described [23]. Total RNA was isolated from cultured astrocytes, oligodendrocyte precursor cells, and granule neurons [24, 25]. The concentration of RNA was determined by optical density on the Nanodrop ND1000 (ThermoFisher).

Quantitative Polymerase Chain Reaction

One microgram of RNA was reverse transcribed to cDNA using the Qiagen SuperScript III RT kit. IR-A/IR-B and IGF-IR were measured using the assay developed by Rowzee et al. [26]. Quantitect real-time primer assays were used for IGF-I, IGF-II, insulin, and IGF-IIR (QT00154469, QT00109879, QT00114289, and QT00177891). Triplicates of samples were amplified using Quantitect SYBR Green Supermix (Qiagen, Valencia, CA, www.qiagen.com) on an ABI Prism 7700 Sequence Detection System (Applied Biosystems, Foster City, CA, www.appliedbiosystems.com) and evaluated using the $\Delta\Delta$CT method.

Laser Microdissection

P5 mouse brains were frozen in isopentane at −30°C. A Zeiss PALM Microbeam was used to collect samples from 15 bilateral medial and lateral SVZ regions. The tissue was collected into Zeiss laser capture caps and the RNA isolated using Arcturus PicoPure (Applied Biosystems).

Western Blotting

Neurospheres were collected, protein extracted, separated, and transferred to nitrocellulose. The blots were probed with anti-

caspase 3 (Cell Signaling, Danvers MA, www.cellsignal.com, 9662; 1:1,000) followed by donkey anti mouse horseradish peroxidase (DAM-HRP) (1:5,000; JacksonImmuno Research) [21].

Retroviral siRNA to the IGF-1R

The RNAi-Ready pSiren-RetroQ-ZsGreen vector from BD Biosciences, San Jose, CA, www.bdbiosciences.com was used to generate a retrovirus to silence IGF-1R gene expression. Oligonucleotides containing a 21-mer RNAi target sequence for the IGF-1R, hairpin loop, terminator sequence, and BamHI/EcoRI restriction sites were synthesized. Sense and antisense oligonucleotides were mixed at a 1:1 ratio, annealed, and then ligated into the vector using T4 DNA ligase. One Shot Top10 chemically competent cells (Invitrogen) were transformed using the ligation mixture. Colonies were collected from carbenicillin plates and screened by restriction digest followed by DNA sequencing.

Nucleofection

Nucleofections were carried out using the Mouse NSC Kit (Cat no. VPG-1004; Lonza Group Ltd., Basel Switzerland, www.lonza.com). Briefly, 5×10^6 tertiary neural progenitor (NP) cells were mixed with 5 μg of purified plasmid DNA, or 5 μg construct and 0.5 μg reporter plasmid cDNA, together with 10 μl of Mouse NSC Nucleofector solution and electroporated using program A-33 in a Nucleofector Amaxa machine.

Immunohistochemistry

Cryostat brain sections of second intron nestin-green fluorescent protein (GFP) mice were collected from p5 animals. Sections were stained using: goat anti-IGF-II (Santa Cruz Biotechnology, Santa Cruz, CA, www.scbt.com; sc-7435 1:200), chicken anti-GFP (Aves Labs Inc. Tigard, OR, www.aveslab.com; GFP-1020, 1:250), and rabbit anti-S100b (DAKO, Carpinteria, CA, www.dako.com; Z0311, 1:250) with 549-DAG, 488-DACh, and Cy5-DAR (Jackson ImmunoResearch). Exposure times for capturing negative controls were identical to the exposure times for the images. Images were assembled into montages using Photoshop CS2.

ESC Culture

Rosa 26 WT ESCs were grown on 0.1% gelatin-coated 10 cm plates on a feeder layer of mitomycin-C treated, mouse embryonic fibroblasts (Millipore). ESCs were cultured in knockout (Invitrogen) media containing 20% ES fetal bovine serum (FBS), 1% Pen-Strep, 1% nucleosides, 0.1 mM 2-mercaptoethanol, and 1,000 units per milliliter ESGRO (Millipore). Media were changed daily and cells were passaged with 0.25% trypsin/EDTA at a 1:5 ratio every 2–3 days. The ESCs were switched to serum-free media (SFM) containing 1,000 units per milliliter of ESGRO and para-amino benzoic acid (0.25 μg/ml), ethanolamine (10 μM), 2-mercaptoethanol (10 μM), sodium selinite (20 nM), fatty acid-free bovine serum albumin (BSA) (9.4 μg/ml), and Apo-transferrin (5 μg/ml) in Dulbecco's modified Eagle's medium-F12 [27]. After one passage, the cells were grown on six-well 0.1% gelatin-coated plates without a feeder layer in SFM at 10,000 cells per well. Cells were grown in one of five SFM variants—two titrated levels of insulin (12.5 μg/ml, 12.5 ng/ml), no insulin or IGF-II (30 nM) or IGF-I + IGF-II. Alkaline phosphatase assays were performed using the Cell BioLabs StemTAG cell staining kit.

Statistical Analysis

Data were analyzed using one-way ANOVA followed by Tukey's post hoc test or Student's t test to detect significant differences between the means with $p < .05$. Analyses were performed using Stat View. Statistical significance was set at p values of <.05.
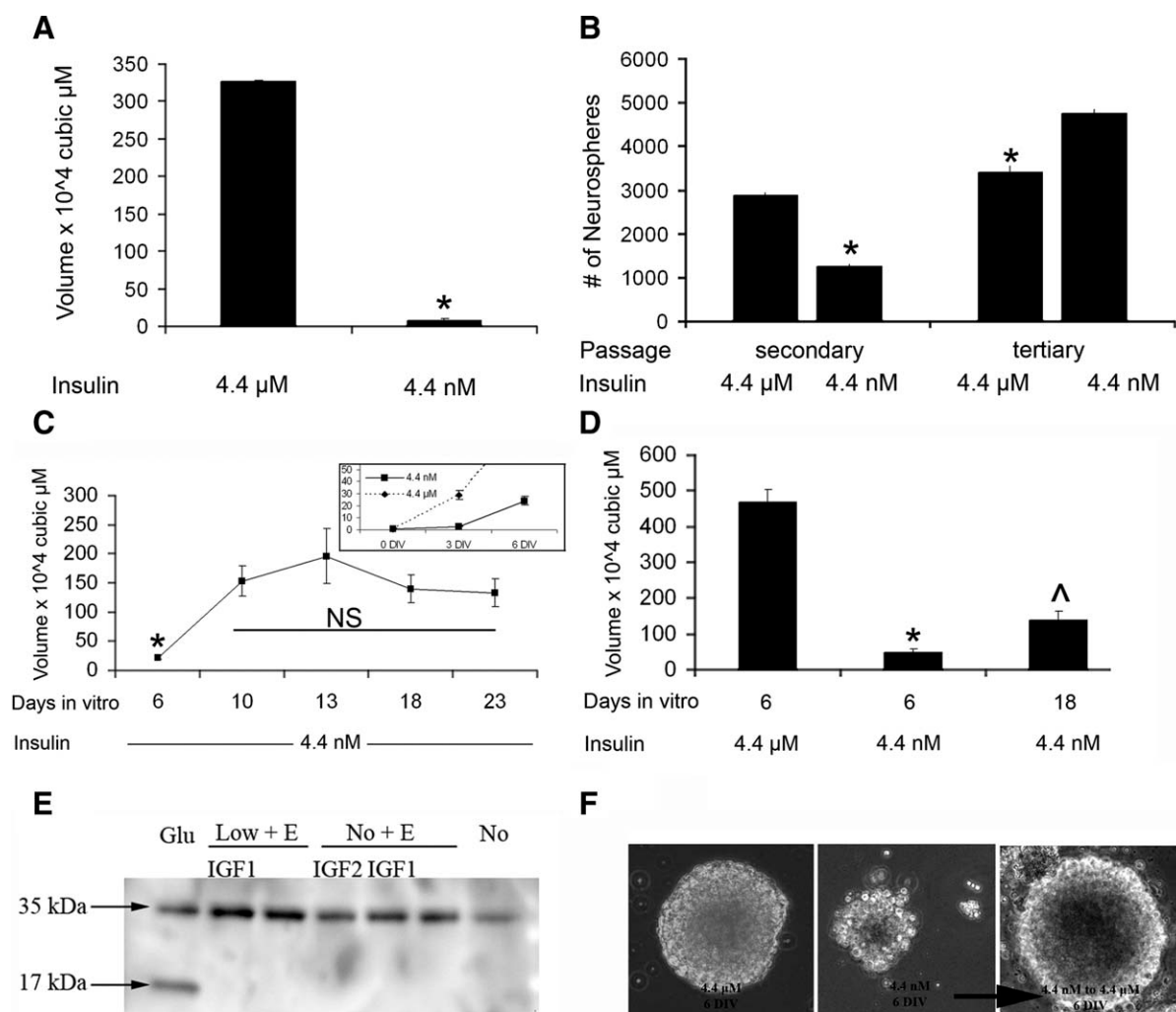
Insulin Level Mediates Neurosphere Growth

Standard media for neurospheres contain micromolar insulin sufficient to activate the IGF-1R as well as the IR. Thus, to evaluate whether IGF-1R signaling might be involved in neurosphere growth, insulin was reduced from 4.4 μM (25 μg/ml) to 4.4 nM (25 ng/ml), a level that stimulates the IR but not the IGF-1R [28]. In the presence of physiological levels of insulin (4.4 nM), both neurosphere size ($7.47 \times 10^4 \pm 0.67$ μm [3]) and number ($1,250 \pm 73.5$) were greatly reduced compared to the control conditions (4.4 μM insulin; $326.8 \times 10^4 \pm 18.5$ μm^3 and $2,875 \pm 72.2$ spheres) (Fig. 1A, 1B). Cell diameters across various conditions did not vary. Upon dissociating and replating the cells at the original density in media containing 4.4 μM insulin, there was no difference in sphere size. However, sphere number increased after passaging neurospheres from 4.4 nM to 4.4 μM insulin, while sphere number decreased after passaging neurospheres generated in 4.4 μM insulin to the same high-insulin media (Fig. 1B, tertiary).

To determine whether the difference in size and number of neurospheres could be attributed to slowed growth, neurospheres were cultured for 18 days in 4.4 nM insulin containing media. Over time, the volume of the spheres grown in 4.4 nM increased slightly but the growth plateaued. Sphere volume peaked at 13 DIV and remained unchanged thereafter (Fig. 1C). Comparing sphere volumes at 18 DIV, the volume of 4.4 nM insulin spheres was significantly smaller than standard 4.4 μM insulin-cultured spheres (Fig. 1D).

To assess whether NSPs were dividing and dying resulting in smaller spheres, neurospheres were cultured in 4.4 nM and standard insulin with EGF for 3 DIV. The spheres were collected and examined by Western blot for active-caspase 3 (Fig. 1E). No cleaved caspase 3 was found, even in neurospheres cultured in no insulin with no growth factors for 3 DIV as compared with a positive control where progenitors were stimulated with 500 μM glutamate (Fig. 1E). To confirm that the reduced insulin was not compromising cell viability, we tested whether growth resumed if spheres in low insulin were transferred back to the standard media. In fact, neurospheres cultured in 4.4 nM insulin resumed growth when transferred to media with 4.4 μM insulin, producing spheres of normal size and appearance (Fig. 1F). Altogether, these studies show that insulin at superphysiological levels promotes growth and proliferation of NSPs but does not affect survival.

IGF System Ligands Differentially Affect NSP Growth

Micromolar levels of insulin can stimulate the IGF-1R (and IGF-1R/IR hybrid receptors) that suggests that either IGF-I or IGF-II will promote the growth of NSPs in 4.4 nM insulin containing media [28]. If this is true, then either IGF-I or IGF-II or a combination of the two factors should mimic the growth as observed when spheres are cultured in standard media. Indeed combining IGF-II and IGF-I together at the maximal doses produced neurospheres that were indistinguishable from control spheres in size (Fig. 2A) and number. To determine the effect of IGF ligands on sphere potentiality, we differentiated spheres grown in the IGF-supplemented media. All conditions produced tripotential spheres, although tripotential spheres were very rare in IGF-I-supplemented medium (Fig. 2A). By contrast, the percentage of tripotential neurospheres was greatest in IGF-II-supplemented medium (57% $\pm$ 3% tripotential in IGF-II and 43% $\pm$ 4% tripotential in IGF-I

Figure 1. Lowering insulin supplementation to physiological levels dramatically reduces neurosphere growth. **(A, B):** Secondary neurospheres were dissociated and grown in medium containing 4.4 μM insulin (the standard concentration referred to as control) or 4.4 nM insulin (a physiological concentration). Epidermal growth factor was present at 20 ng/ml. Cells were cultured for 6 DIV to enable sphere formation. Sphere volume (A) and number (B) were quantified with results expressed as means $\pm$ SEM. Neurospheres were passaged and replated to evaluate self-renewal (B). **(C):** To determine whether the smaller sphere size was simply a matter of growth rate, spheres were grown for up to 23 DIV. Inset depicts spheres grown in 4.4 nM insulin versus 4.4 μM insulin over 6 days. **(D):** Spheres volumes at 6 or 18 DIV in physiological and superphysiological insulin. **(E):** Neural stem/progenitor cells (NSPs) were cultured for 3 DIV in 4.4 μM insulin and then transferred to either no insulin or 4.4 nM insulin $\pm$ growth factors for 3 DIV prior to protein collection and Western blot analysis for active casapase 3. **(F):** NSPs were cultured for 6 DIV in 4.4 nM insulin and then transferred to 4.4 μM insulin, and compared to NSPs cultured in 4.4 μM for 6 DIV.*, $p < .05$; ^, $p < .01$ by ANOVA or Student's t test. Abbreviations: ANOVA, analysis of variance; DIV, days in vitro; IGF, insulin-like growth factor; N.S., not significant.

and IGF-II vs. 19% $\pm$ 4% tripotential in 4.4 μM insulin) (Fig. 2A).

To determine whether IGF-II promoted self-renewal of the NSPs, a limiting dilution analysis (LDA) was performed (Fig. 2B). Spheres were grown in the test conditions, dissociated, and then plated at varying densities in standard media as described previously [29]. After 6 DIV, individual wells for each group were examined for the presence of spheres ($n = 6$ wells per experiment, with a minimum of three experiments). These LDA experiments showed that the highest proportion of sphere-forming cells was obtained in 4.4 nM insulin and 4.4 nM insulin plus IGF-II (one in 4,200 and one in 4,200 cells per centimetre square, respectively) as compared to control or 4.4 μM insulin (one in 6,100 cells per centimetre square). Growth in 4.4 nM insulin with IGF-I and IGF-II (one in 10,000 cells per centimetre square) resulted in lower proba-

bilities of sphere formation. Higher probabilities of sphere formation correlate with higher percentages of tripotential spheres. Since 4.4 nM insulin and 4.4 nM insulin plus IGF-II had higher percentages of tripotential spheres and better probabilities for sphere formation, we evaluated them over multiple passages after initial growth and compared growth to the control, 4.4 μM insulin (Fig. 2C, 2D). Sphere number per well for 4.4 nM insulin with IGF-II increased across passages and remained elevated as compared to 4.4 nM insulin and 4.4 μM insulin (Fig. 2C). Additionally, the absolute number of spheres obtained continued to expand by a factor of 2.5 per passage for cells maintained in 4.4 nM insulin with IGF-II, whereas sphere number for 4.4 μM insulin remained nearly constant and the 4.4 nM insulin decreased slightly (Fig. 2D).

We evaluated expression of several stem cell genes, ABCg, FABP7, and Sox1, by Q-PCR using RNA isolated
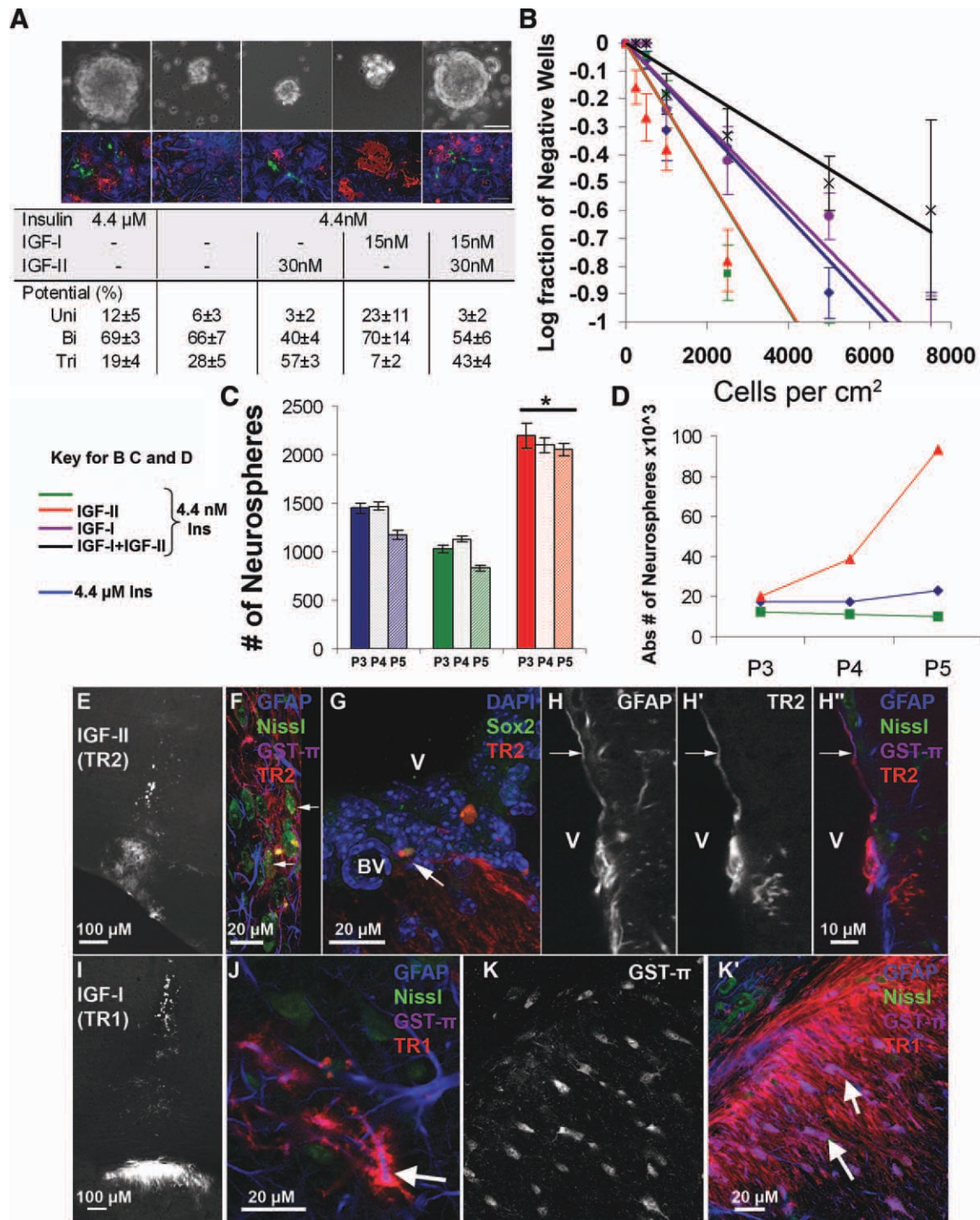
Figure 2. IGF-II increases tripotential neurospheres and sphere formation. **(A):** Medium was supplemented with 15 nm IGF-I, 30 nM IGF-II, and 20 ng/ml epidermal growth factor (EGF) in physiological insulin. Representative spheres taken at ×10 magnification and grown as indicated (scale bar = 50 µM), first row. Spheres were differentiated in control medium with serum and no growth factors for 6 days in vitro (DIV), second row. Immunohistochemistry (IHC) for oligodendrocytes (O4, red), astrocytes (GFAP, blue), and neurons (TuJ1, green) was performed to identify the potentiality of the sphere (scale bar = 50 µM), and the types of spheres were quantified and expressed as a percentage of total (table). Potentiality of the spheres was scored according to the number of cell types formed from a single sphere after differentiation, with unipotent, bipotent, and tripotent referring to one, two, or three cell types, respectively. **(B):** Limiting dilution analysis was performed on spheres passaged from the conditions in A. Cells were plated at the various dilutions in 96-well plates, and the fraction of negative wells was scored. A linear fit was plotted for each condition, 4.4 µM (blue), 4.4 nM insulin (green), or 4.4 nM insulin with 30 nM IGF-II (red), 4.4 nM insulin with 15 nM IGF-I (yellow), and 4.4 nM insulin with IGF-I and IGF-II (black) all with EGF at 20 ng/ml, error bars are SEM, all intercepts were found significantly different by linear regression analysis. **(C):** Cells in 4.4 µM (blue) or 4.4 nM insulin (green) or 4.4 nM insulin with 30 nM IGF-II (red) all with EGF at 20 ng/ml were passaged and maintained in the same media over four passages at 30,000 cells per well. Number of cells per well across passages is graphed (*n* = 3 independent experiments). **(D):** Absolute number of cells for a representative experiment across passages is graphed. **(E):** IGF-II-treated cells (TR2) 1 month after transplantation **(E–H)**. (F): TR2/Nissl neurons (arrows). (G): Sox2, TR2, and Dapi cells adjacent to the V and BV. (H″): TR2/GFAP cell with process contacting V (H; GFAP) (H′; TR2). (H, I): IGF-I-treated cells (TR1) 1 month after transplantation **(I–K)**. (J): TR1/GFAP cell in cortex (arrow). **(K′):** TR1/GST-π cells bodies (GST-π; K). Abbreviations: BV, blood vessel; GFAP, glial fibrillary acidic protein; IGF, insulin-like growth factor; V, ventricle.

from spheres grown for 6 DIV in the test conditions (Supporting Information Table S1). ABCg, FABP7, and Sox1 were higher for NSPs grown in 4.4 nM insulin with IGF-II versus control (greater than 1.7-fold). IGF-I did not produce any significant changes from the control for these stem cell genes. Prior to the extensive evaluation of the effects of IGF-I and IGF-II on the NSPs, we preformed dose-effect response curves to find the maximal doses of IGF-I and IGF-II on the neurospheres. Dose-effect curves were generated by supplementing IGF-I and IGF-II at $1\times$ (2 nM, 3.8 nM) and $8\times$ (15 nM, 30 nM), the K_D of the either IGF-I or IGF-II for IGF-1R in the presence of 20 ng/ml EGF into the medium (Supporting Information Fig. S1). After 6 days of growth, neurosphere size and number had increased slightly with the IGF-I addition compared with the 4.4 nM insulin condition, but IGF-I did not restore growth to the same level as 4.4 μM control (Supporting Information Fig. S1A, S1B). When 4.4 nM insulin media were supplemented with either IGF-II at $1\times$ (3.8 nM) or $8\times$ (30 nM), its K_D for IGF-1R, neurosphere number increased as the concentration of IGF-II increased. Addition of 30 nM IGF-II restored the number of neurospheres observed in the control condition (Supporting Information Fig. S1D). Over the 6 days, neurosphere size increased slightly but was 65% smaller in the presence of IGF-II than in controls. As 30 nM IGF-II restored neurosphere number to that observed in control conditions, this concentration of IGF-II was used for all IGF-II experiments.

To more fully assess the developmental potentials of neural precursors propagated in IGF-I versus IGF-II, NSPs were generated in medium containing either 4.4 μM insulin, 30 nM IGF-II, or 15 nM IGF-I for 6 DIV. They were then transplanted into the neocortices of p21 mouse brains and their fate assessed after 1 month in vivo (Fig. 2E, 2I). NSPs propagated in IGF-II-supplemented medium upon differentiation in the neocortex formed astrocytes, oligodendrocytes, and neurons (Fig. 2F) similar to control-treated cells (data not shown). In addition, a subset of cells propagated in IGF-II-supplemented medium migrated to periventricular locations. These cells were Sox-2+ and they extended processes to blood vessels (Fig. 2G, arrow) as well as GFAP+ processes that contacted the lateral ventricle (Fig. 2H). These periventricular cells were only found in the recipients of IGF-II-treated cells. Astrocytes (Fig. 2J) and oligodendrocytes, but no neurons, were observed in the brains that received IGF-I-treated cells. Cells maintained in growth medium supplemented with IGF-I did not colonize periventricular domains. Instead, they populated the white matter tracts. Consistent with an oligodendroglial identity, these cells were immunostained for glutamine S-transferase (GST)-π and possessed long, thin processes that ran parallel to and adjacent to subcortical axons (Fig. 2K').

Multiple IGF-II Signaling Receptors Are Expressed in NSPs

Our data suggested that IGF-II was more potent than IGF-I due to the ability of IGF-II to sustain neurosphere number across passages, to sustain the tripotentiality of the spheres, and its ability to increase the expression of three stem cell genes, while IGF-I supplementation resulted in the lowest percent tripotentiality, low sphere-forming frequency in the LDA assay, and no change in stem cell genes. One difference between IGF-II and IGF-I that could explain this unique action of IGF-II is that IGF-II binds the IR-A with high affinity. A prediction from this hypothesis is that primitive neural precursors would express higher levels of IR versus IGF-1R as compared to other more lineage restricted cell types. To measure levels of IR-A, IR-B, and the IGF-1R, we used a

Q-PCR assay recently developed for relative mRNA quantification for these receptors [26].

IR-A was the most highly expressed receptor in NSPs (Fig. 3A). Additionally, the high expression level of IR-A was unique to the NSPs and was found at successively lower levels in developmentally more restricted neural cells, with neurons expressing the lowest levels of IR-A. When the level of IR-A was expressed as a ratio to IR-B or IGF-1R, IR-A was 5.8 times more abundant than IR-B and six times more abundant than IGF-1R in neurospheres, whereas astrocytes and oligodendrocytes displayed almost equal expression of both IR-A and IR-B (Fig. 3B). An unexpected finding was the lack of IR-B in neurons.

We also evaluated the expression of IGF-2R (Fig. 3A, inset). Q-PCR demonstrated that IGF-2R is expressed by all cell types at equivalent levels. The availability of IGFs to bind to cells is further regulated by the IGFBPs. As our previous dose-effect curves required higher levels of the growth factors than would be expected based on the binding affinities of the ligands for their receptors, we hypothesized that NSPs produce IGFBPs. Consistent with this hypothesis, we found that neurospheres express IGFBP2, and to a lesser extent, IGFBP3 (Fig. 3C).

The choroid plexus produces and secretes IGF-II throughout the lifespan [30]. It is also known that the NSCs extend processes through the ependymal layer to contact the CSF [9]. Immunohistochemistry for IGF-II in situ showed that IGF-II is highly expressed in the choroid plexus and that there appears to be a gradient of IGF-II within the SVZ where the highest levels are in regions adjacent to the ventricles (Fig. 3D, left). Analyses of transgenic mice expressing GFP from the second intron of the nestin promoter (to label NSCs) revealed GFP+ cells along the wall of the lateral ventricle, surrounded by punctate IGF-II staining (Fig. 3D, top right). Since IGF-II is highly abundant in vivo, it was of interest to compare levels of IGF-II with the other receptors and ligands in the system. The levels of IR-A, IR-B, and IGF-1R in subregions of the SVZ were examined by laser capture and Q-PCR from samples obtained from coronal brain sections. Confirming the nature of the cells within the samples collected, the most medial region of the SVZ contained high Sox1 and lacked Olig1 expression, whereas the lateral SVZ had 50% reduced expression of Sox1 and high expression of Olig1 (data not shown). IR-A was elevated in the medial SVZ, whereas IGF-1R was reduced (Fig. 3E, 3F). The lateral SVZ had equal levels of the receptors reflecting the in vitro data. Unexpectedly, both regions lacked IR-B expression. In parallel studies, the levels of IGF-II, insulin, and IGF-I mRNA in both P5 and 2-month-old adult choroid plexus and SVZ tissue were measured by Q-PCR. High levels of both IGF-II and insulin mRNA and very low levels of IGF-I (not shown) were present in the tissue (Fig. 3G). We also evaluated these mRNAs in the various cell types differentiated in vitro (Fig. 3H). Neurospheres produced low to almost negligible levels of all ligands (IGF-I 0.16, IGF-II 0.016, and insulin 0.13). However, IGF-I and insulin mRNA were present in astrocytes (1.1 and 0.95, respectively), and oligodendrocytes had extremely high levels of IGF-I mRNA (7.6). One interesting note was the presence of IGF-II mRNA in the granule neurons.

## IGF-II Promotes NSP Self-Renewal Independent of IGF-1R

As IR-A was most abundant in comparison to either IGF-1R or IR-B in NSPs and in the SVZ, we hypothesized that IGF-II acting via the IR-A might uniquely regulate NSC self-renewal. Therefore, we decreased IGF-1R by shRNA knockdown and a specific blocking antibody that causes the
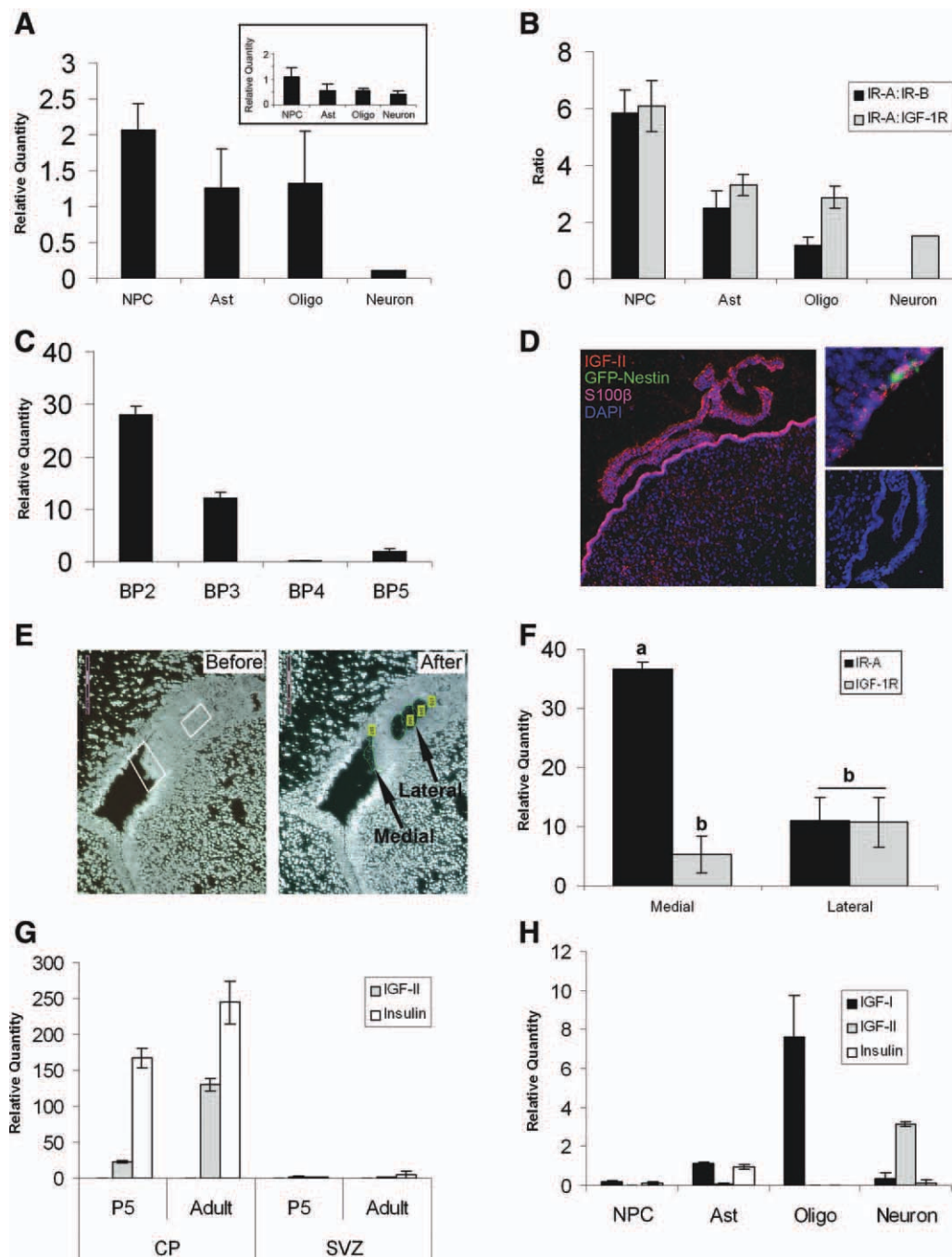
Figure 3. IR-A is predominantly expressed by NSPs in comparison to more differentiated cell types. mRNA was isolated from neurospheres, astrocytes, oligodendrocytes, and granular neurons in order to examine the receptor and ligand expression. **(A, B):** IR-A, IR-B, IGF-1R, and IGF-2R expressions in the various cell types were measured using a Q-PCR assay. Relative quantity (RQ) of IR-A for the various cell types and IGF-2R (inset) (A) shows elevated level of IR-A. A ratio comparing the IR-A to either IR-B or IGF-1R in each of the cell types gives a representation of receptor profile for the varying cell types by showing the abundance of IR-A to the other receptors (B). **(C):** Q-PCR showing the RQ of the insulin-like growth factor binding proteins in neurospheres. **(D):** Immunohistochemistry of the lateral ventral and CP for S100β (purple), IGF-II (red) and Dapi (blue) (left panel), and GFP-Nestin (green) (right top panel) of SVZ shows punctate IGF-II staining in the CP and into the SVZ. Negative control (bottom right panel). **(E):** Laser capture microdissection of the medial and lateral SVZ. **(F):** The RQ values for IR-A, IR-B (undetectable), and IGF-1R were graphed. **(G):** The RQ values for IGF-II and insulin in P5 and adult tissues. **(H):** mRNA for IGF-I, IGF-II, and insulin was also examined in the cell types. Abbreviations: CP, choroid plexus; GFP, green fluorescent protein; IGF, insulin-like growth factor; IR, insulin receptor; NPC, neural progenitor cell; SVZ, subventricular zone.

internalization and degradation of the IGF-1R and IMC-A12 [31]. Both approaches produced similar results, although the blocking antibody was more effective (Fig. 4) and produced neurospheres that were smaller in size (less than 1/10 the size of control spheres) reminiscent of the growth deficiency observed when spheres were maintained in 4.4 nM insulin (Fig. 4A–4C); however, sphere number was unaffected (Fig. 4D, 4E).
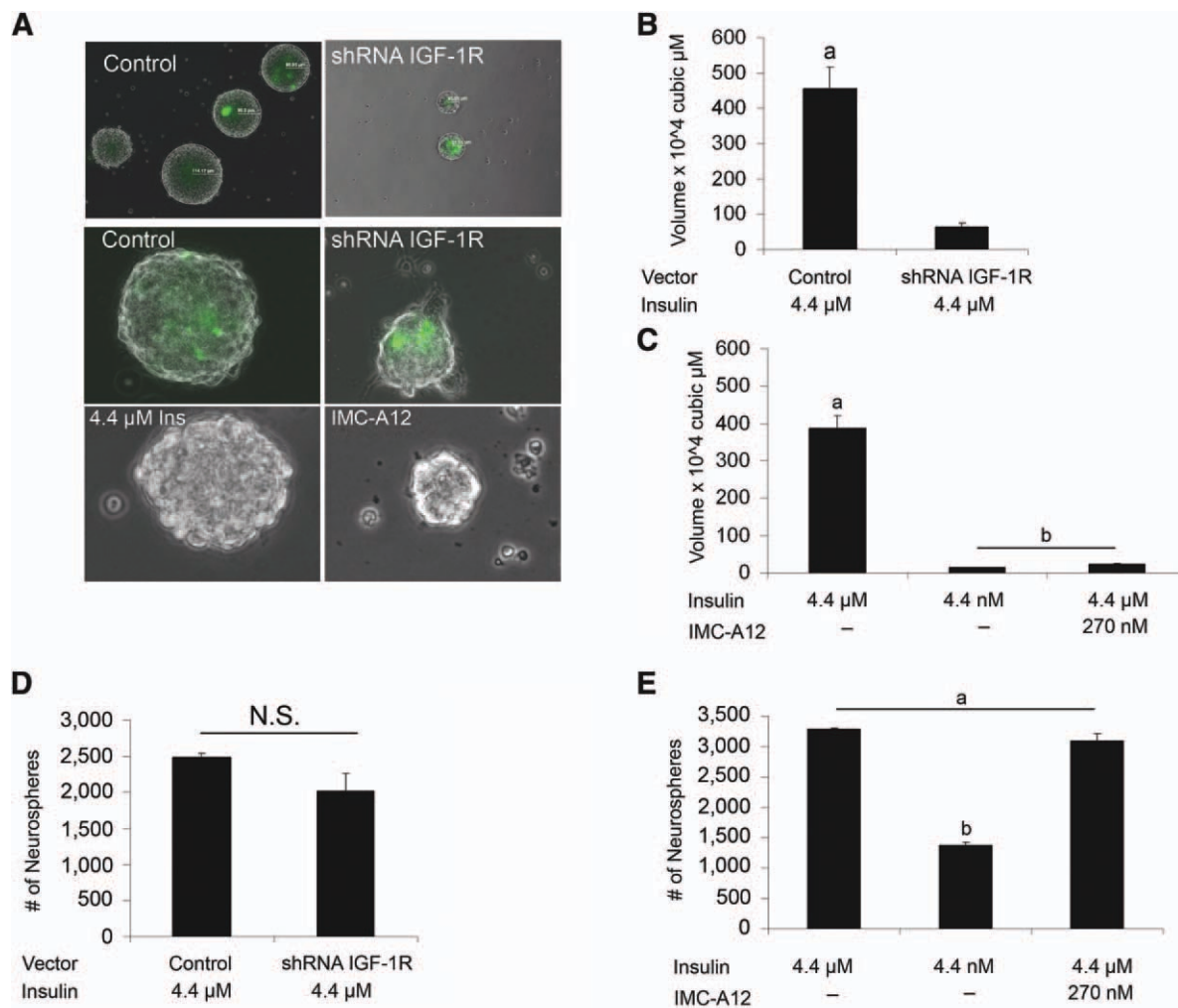
Figure 4. IGF-1R effects neurosphere volume not number. IGF-1R was manipulated with either an shRNA to reduce IGF-1R expression (**A, B, D**) or a blocking antibody, IMC-A12, to block IGF-1R (**C, E**). Neurospheres were dissociated and single cells were transfected with a plasmid containing both a zs green reporter and an shRNA against IGF-1R. Cells were cultured in control medium for 6 days in vitro (DIV) to enable sphere formation. Green spheres were examined, and sphere volume (B) and number (D) were quantified with results expressed as means ± SEM. (A, C, E): Additionally, the action of IGF-1R was blocked by IMC-A12. Representative spheres from both knockdown and blocking of IGF-1R (A). The action of insulin via IGF-1R was blocked by use of IMC-A12. Secondary neurospheres dissociated and grown in medium containing control insulin with IMC-A12 and compared to physiological and control insulin conditions. Cells were cultured for 6 DIV to enable sphere formation, and volume (C) and number (E) were assessed. Knockdown and blocking of IGF-1R results in reduced volume similar to neurospheres cultured in 4.4 nM insulin but does not affect number. ANOVA with Tukey's post hoc, a, b, and c denote groups with $p < .05$. Abbreviations: N.S., not significant; IGF, insulin-like growth factor.

Since manipulating the IGF-1R only partially modeled the effect of reduced insulin or IGF-II, we examined the roles of the other receptors of the IGF system. We hypothesized that the IGF-1R was dispensable for the effects of IGF-II on NSP self-renewal. To test this hypothesis, we grew NSPs in IGF-II-supplemented media in the presence of IMC-A12 antibody to block IGF-1R. This experiment was performed in 4.4 nM insulin so that the effects of IGF-II could be readily observed. Supporting the hypothesis that IGF-1R does not effect self-renewal, sphere number was unaffected by the addition of IMC-A12 (Fig. 5B).

IR Mediates NSC Self-Renewal

To more directly assess the role of IR on neurosphere growth, we manipulated IR levels using an shRNA for the IR [32]. The IR difference between IR isoform A and B is 12 amino acids and results from the deletion of exon 11 from isoform A. Because of the small difference between the isoforms, no

reagents exist to distinguish the isoforms at the protein level, and there is no way to selectively knockdown the individual isoforms. Since IGF-II has selective affinity for IR-A and NSPs express more IR-A than IR-B, we tested whether knocking down the IR abrogated the IGF-II effects on NSPs. Confirming our predictions, fewer spheres formed in the presence of the IR shRNA and some cells that labeled for IR (GFP+) remained as single cells and did not form spheres (Fig. 6A, 6B). Analogously, growing NSPs over multiple passages in the presence of an IR function-blocking antibody reduced neurosphere number upon passaging the cells (Fig. 6C). Moreover, the IR blocking antibody inhibited tripotential colony formation upon cell differentiation. When cells were cultured in medium devoid of insulin, a few tiny spheres formed but most cells remained as single cells. Interestingly, cells cultured without insulin but with the addition of IGF-II, or IGF-I plus IGF-II, formed spheres indistinguishable from control spheres in terms of size and number (Fig. 6D).
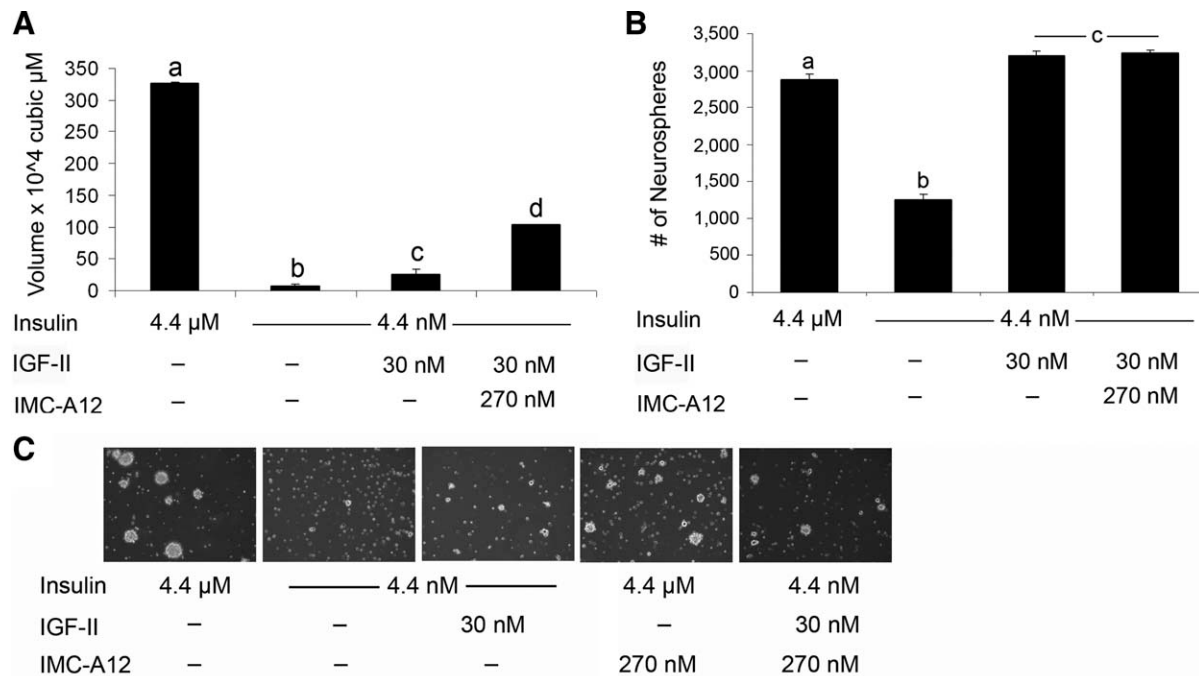
Figure 5. Insulin-like growth factor (IGF)-II actions are independent of IGF-1R and IGF-2R. **(A, B):** Secondary neurospheres were dissociated and grown in media with varying insulin and IGF-II. IMC-A12 was added to block actions of IGF-II via IGF-1R. After 6 days in vitro, sphere volume (A) and number (B) were analyzed with results expressed as means ± SEM, a, b, c, and d denote groups as determined by ANOVA with Tukey's post hoc $p < .05$. **(C):** Representative ×10 magnification fields from CTL, 4.4 nM, IGF-II, CTL insulin with IMC-A12, and IGF-II + IMC-A12 (left to right, respectively). Note the increase in number and how it is maintained when IGF-1R binding and IGF-2R are blocked, while the number remains elevated and unaffected.

Superphysiological Insulin Is Not Important for Murine ESC Culture

To determine whether our observations carried over to other stem cell cultures, we examined the role of micromolar insulin in murine ESC cultures. As all of the commercially available ESC media contain at least 10 μM insulin, we adapted a medium described by Furue et al. [27]. Medium supplemented with LIF with either no insulin 12.5 nM or the standard 12.5 μM insulin was used to culture mouse ESCs (mESCs). Pluripotency gene expression was evaluated by Q-PCR. Contrary to our expectations, mESCs could be maintained over multiple passages in medium lacking insulin and appeared similar to cells grown with feeder cells in standard ESC medium (Fig. 7A). Q-PCR analysis for Oct4, Sox2, and Nanog showed no differences in expression from early to late passage in any of the conditions compared to control ESCs cultured with a feeder layer (Fig. 7B). Alkaline phosphatase showed no differences between the cultures (Fig. 7C).

CONCLUSION

The results of our studies indicate that IGF system activation is necessary for neural stem/progenitor cell growth. Both IGF-II and one of its receptors, IR-A, are abundant within the NSC niche in vivo. In vitro, IGF-I and II cooperate to maintain NSC numbers and the NSC's ability to self-renew. IGF-I maintains NSC numbers by promoting cell division (via the IGF-I receptor), whereas IGF-II promotes the expression of proteins essential for NSC self-renewal and 'stemness' (via the insulin receptor).

DISCUSSION

Our studies demonstrate that IGF-I and IGF-II exert distinct effects on SVZ neural precursors, with IGF-II acting via IR to maintain NSCs and IGF-I acting through IGF-1R to stimulate progenitor cell proliferation. We found that: (a) IGF system activation is necessary for neural progenitor proliferation but not survival, (b) neural progenitors express high amounts of IR-A in comparison to other cell types, (c) a gradient of IGF-II is present in the NSC niche in vivo, (d) IGF-II maintains NSC number via IR-A, (e) IGF-I via IGF-1R stimulates progenitor cell proliferation, and (f) mESCs do not require IGF system activation for maintenance or proliferation.

SVZ NSCs Require IGF System Activation

Stem cells in various organisms depend on insulin and insulin-like peptides for their growth and maintenance. In *Drosophila*, insulin affects neurogenesis [33], and *Drosophila* insulin-like peptides (DILPs) act directly on germline stem cells along with factors in their niche to enable their proliferation [34]. DILPs also control germline stem cell maintenance by controlling cap cell number via Notch and E-cadherin [35]. Zebrafish also depend on insulin for stem cell and NSC maintenance. Zebrafish have two functional IR genes, *insra* and *insrb*, which are functional homologs of human IR. Knocking down *insra* in zebrafish causes developmental defects in the central nervous system (CNS). The midbrain is smaller, boundaries within the hindbrain are disrupted, the forebrain is smaller, and the retina is disorganized and undifferentiated [36]. Similarly, disrupting Steppke, the downstream signal for insulin in *Drosophila*, reduces organism size [37]. Our studies demonstrate that mammalian NSCs depend
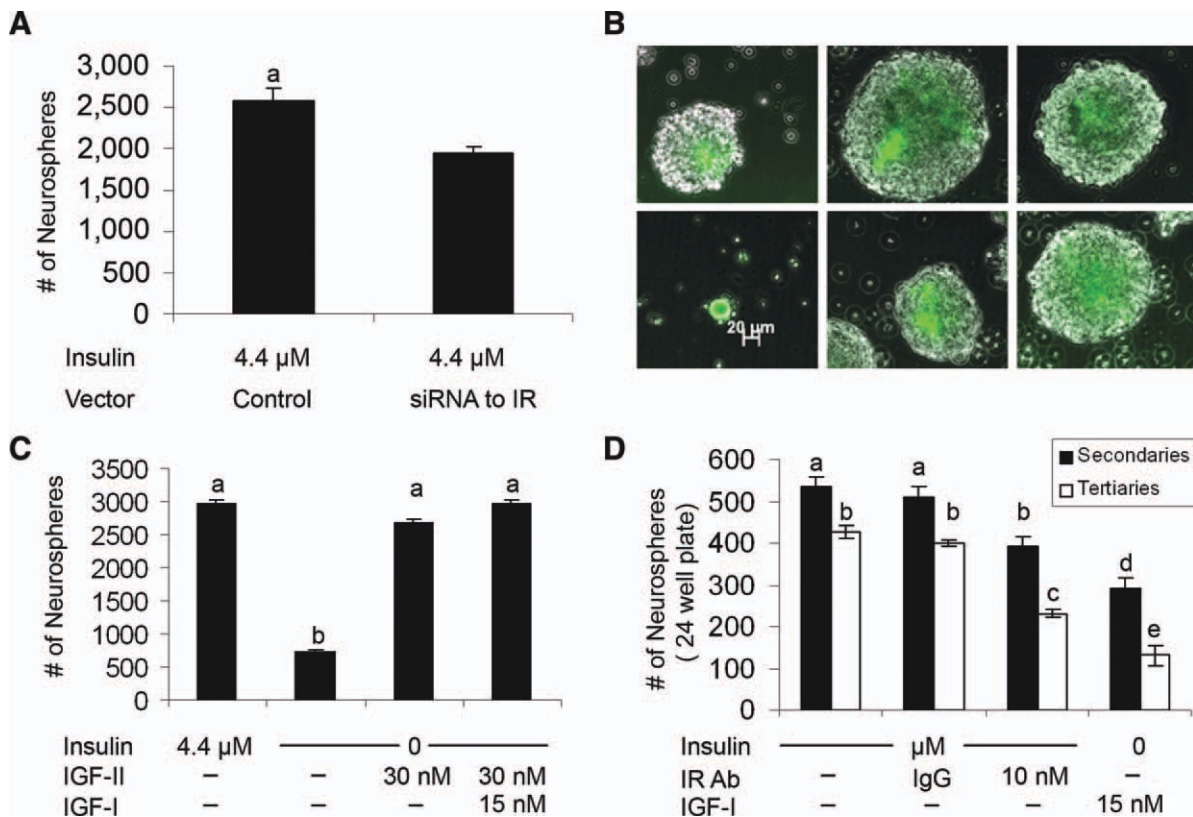
Figure 6. IR effects neurosphere number. **(A, B):** A plasmid containing an shRNA to IR and a plasmid containing a zs green reporter were cotransfected into dissociated neurospheres and allowed to grow in control media for 6 days in vitro (DIV) to enable sphere formation. Neurosphere number (A) of green spheres was analyzed. Representative spheres after transfection are shown (B). **(C):** Secondary neurospheres were dissociated, and cells were cultured in no insulin, or no insulin with IGF-II or IGF-I and IGF-II all with 20 ng/ml EGF for 6 DIV to enable sphere formation. **(D):** Numbers of secondary and tertiary spheres obtained with IR blocking antibody addition or with only IGF-1R stimulation (no insulin + IGF-I). Sphere number (C, D) was quantified with results expressed as means $\pm$ SEM. Significant differences were determined by Student's t test (A) $p < .05$, or ANOVA followed by Tukey's post hoc $p < .05$ a, b (C) and $p < .001$ a–e (D) letters denote groups. Abbreviations: IGF, insulin-like growth factor; IgG, immunoglobulin G; IR, insulin receptor.
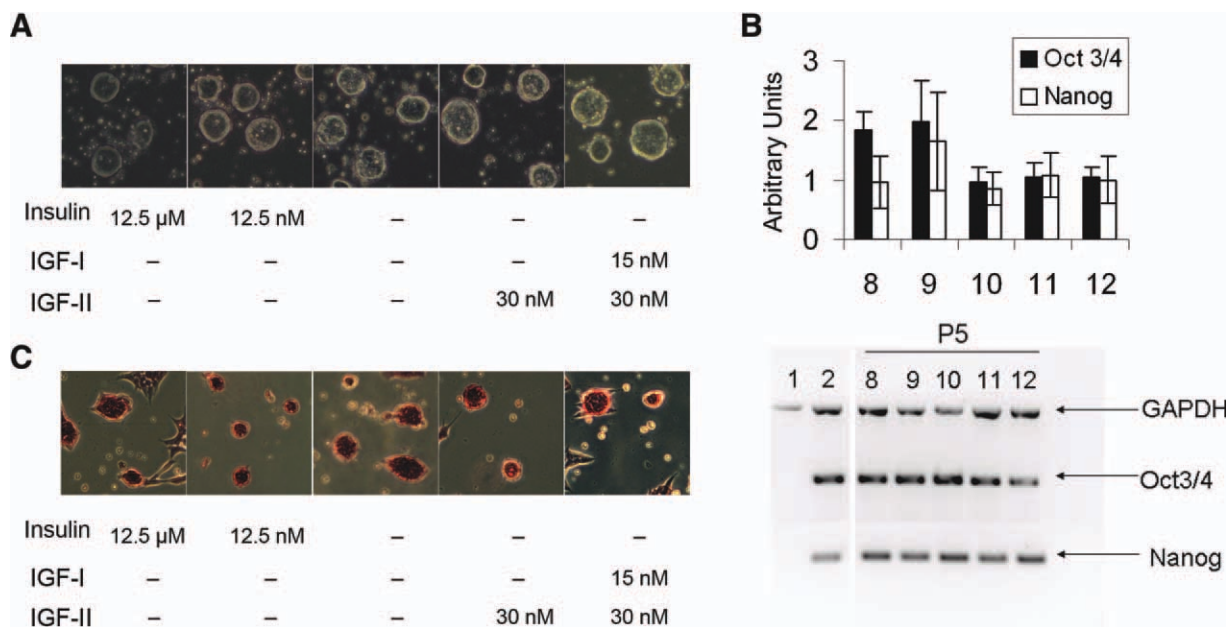
Figure 7. Mouse embryonic stem cells (mESCs) do not require IGF system activation for growth. mESCs were cultured in chemically defined media with 12.5 μM or 12.5 nM insulin, no insulin or no insulin with IGF-II or IGF-I and IGF-II. **(A):** Representative $\times$10 magnification images showing round morphology of pluripotent cultures in various media conditions. **(B):** Semiquantitative real-time PCR for Oct3/4 and Nanog for mESCs grown in various media conditions. Top, graph depicts levels normalized to GAPDH. Bottom, image of representative gel used to determine relative levels. 1. Murine embryonic feeder cells (negative control). 2. Rosa26 cells (positive control). Lanes 8-12 passage 5 (P5). 8. No insulin. 9. 12.5 nM insulin. 10. No insulin with IGF-II. 11. No insulin with IGF-I and IGF-II. 12. 12.5 μM insulin. GAPDH was run as a housekeeping gene and reaction stopped at 22 cycles while Oct3/4 and Nanog were stopped at 28 cycles. **(C):** Representative images showing alkaline phosphatase staining of colonies in various media conditions. Abbreviations: GAPDH, glyceraldehyde 3-phosphate dehydrogenase; IGF, insulin-like growth factor.

upon insulin and IR-A signaling for neurogenesis and CNS development. Thus, IGF system activation appears to be a conserved mechanism for stem cell maintenance.

Stem Cell Populations Differentially Respond to the IGF System Ligands

IGF-I and IGF-II uniquely affect the growth, proliferation, and maintenance of the NSP cell population. IGF-I promotes progenitor cell proliferation, whereas IGF-II promotes NSP maintenance (Fig. 2). IGF-I achieves its actions through IGF-1R while IGF-II acts through IR-A. When IGF-1R is blocked or knocked down, sphere size but not number is reduced (Fig. 4). The volume of a sphere is a reflection of the accumulation of cells as a result of cell divisions. Since manipulating IGF-I and IGF-1R affected sphere size, IGF-1R activation appears to increase neural progenitor proliferation. While both IGF-I and IGF-II bind IGF-1R with high affinity, IGF-II was not able to restore sphere volume as IGF-I did but IGF-II was able to restore sphere number. The same effect could be achieved by knocking down the IR (Fig. 6). Additionally, when IGF-II was forced to act via IR-A, it exerted the same effects as when it could act freely on the cell (Fig. 5). Since IR-A expression is higher in the NSC niche and in NSPs compared to lineage restricted cells, and since IGF-II promotes NSP expansion, IGF-II and IR most likely exert their effects on the stem cells rather than the progenitors. Confirming this prediction, NSPs propagated in IGF-II-supplemented medium migrated to and colonized periventricular loci where they possessed both the morphology and markers of bona fide adult NSCs. By contrast, NSPs maintained in IGF-I, instead of migrating to periventricular sites, predominantly colonized white matter tracts where they produced oligodendrocytes and astrocytes. These results indicate that cell culture conditions can be tailored to promote NSCs versus glial progenitors for regenerative medicine applications.

NSPs grow in 4.4 μM insulin, but the number of NSPs obtained is greater in IGF-II-supplemented media; therefore, IR stimulation is necessary for NSP growth; however, NSC self-renewal is more effectively obtained when IGF-II rather than insulin activates the IR. This is most likely the consequence of differential signaling by insulin and IGF-II through IR-A. Consistent with this conclusion, IGF-II was a more potent mitogen than insulin in a study comparing the effects of insulin and IGF-II on murine fibroblasts that only expressed IR-A, and the gene expression profiles of the two ligands differed [38]. IGF-II more potently activated p70S6K and persistent ERK1/2 phosphorylation, whereas insulin via IR-A resulted in longer Akt activation [39]. These data support the view that IGF-II and insulin activate IR-A distinctly.

The difference in IGF-I and IGF-II function is consistent with their endogenous expression and prior studies on IGF-I function. IGF-II is highly expressed in the niche predominantly from choroid plexus, whereas IGF-I is expressed at low levels in the niche. However, IGF-I is expressed by astrocytes and oligodendrocytes. Previous research has postulated a role for IGF-I as a differentiation inducing agent during gliogenesis due to its lack of presence in the ependymal lining and choroid plexus and sparse labeling around the SVZ [40]. This parallels our finding that IGF-I only stimulated neurosphere volume in the presence of IGF-II, reduced the number of tripotential spheres, and produced a low sphere-forming frequency. In a study that appeared while our manuscript was under review, the IGF-1R was shown to be involved in fetal neural progenitor cell proliferation [41]. These investigators also showed binding of IGF-II to cells surrounding the lateral ventricle (LV) and concluded that IGF-II binding to the IGF-1R was necessary for neural progenitor cell proliferation. Our data provide empirical data to support

their conclusions, but more importantly extend their observations by establishing that IGF-II binds to IR-A to promote NSC self-renewal. A study by Chen et al. showed that IGF-II enhanced memory formation [42]. However, the possibility that IGF-II was acting through the IR-A was not investigated.

IGF-II Is Required for Adult but Not ESCs

IGF-II has been implicated in human ESC (hESC) self-renewal, maintenance, and growth. IGF-II is produced by hESC-derived fibroblast-like cells, whereupon it has been suggested to activate IGF-1R in hESC to promote their survival and self-renewal [43]. However, a more recent study has shown that hESCs can be maintained in conditioned media from mesenchymal stem cells that lacks IGF-II. Furthermore, neutralizing IGF-II had no effect on proliferation, growth, overall morphology, or gene expression [44]. In our experiments, IGF-II was a potent stimulator of NSPs, a tissue specific stem cell, but we failed to establish a requirement for IGF-II, IGF-I, or even insulin for the growth of murine ESCs (Fig. 7). Therefore, it appears that ESCs and tissue-specific NSCs have different requirements for IGF system activation. Data from IGF system null mutant mice support the conclusion that IGF-II is not required for early embryogenesis, but it is required for organ and body growth beginning at day E9/10, resulting in pups ~60% of normal size at birth [45, 46]. Additional studies in IR gene disrupted mice point to a role for the growth-mediating effects of IGF-II [46–49]. IR null mutant mice display growth defects in late embryogenesis, and IGF-1R/IGF-II and IGF-1R/IR null double mutants are phenotypically indistinguishable [49]. Furthermore, studies of paternal IGF-II null mice suggest that IGF-II levels at E9/10 determine organism size [45]. Taken together, these data suggest the blastocyst forms properly; however, there are developmental issues when IGF-II is perturbed.

The possible difference between embryonic and adult stem cells and the requirement for IGF system activation warrants further study. We have shown that murine NSPs require IGF-II stimulation of IR-A for stem cell maintenance. Insulin alone enables limited cell proliferation, but it does not maintain stem cell homeostasis. Our studies also highlight IGF-II as an important factor in the niche. IGF-II is highly abundant in the choroid plexus and is secreted into the CSF, which must be considered as a component of the NSC niche.

DISCLOSURE OF POTENTIAL CONFLICTS OF INTEREST

The authors indicate no potential conflicts of interest.

REFERENCES

1   Mirzadeh Z, Merkle FT, Soriano-Navarro M et al. Neural stem cells confer unique pinwheel architecture to the ventricular surface in neurogenic regions of the adult brain. Cell Stem Cell 2008;3:265–278.

2   Lim DA, Tramontin AD, Trevejo JM et al. Noggin antagonizes BMP signaling to create a niche for adult neurogenesis. Neuron 2000;28:713–726.

3   Kerever A, Schnack J, Vellinga D et al. Novel extracellular matrix structures in the neural stem cell niche capture the neurogenic factor fibroblast growth factor 2 from the extracellular milieu. Stem Cells 2007;25:2146–2157.

4   Zheng W, Nowakowski RS, Vaccarino FM. Fibroblast growth factor 2 is required for maintaining the neural stem cell pool in the mouse brain subventricular zone. Dev Neurosci 2004;26:181–196.

5   Campos LS, Decker L, Taylor V et al. Notch, epidermal growth factor receptor, and beta1-integrin pathways are coordinated in neural stem cells. J Biol Chem 2006;281:5300–5309.

6   Bultje RS, Castaneda-Castellanos DR, Jan LY et al. Mammalian Par3 regulates progenitor cell asymmetric division via notch signaling in the developing neocortex. Neuron 2009;63:189–202.

7   Costa MR, Wen G, Lepier A et al. Par-complex proteins promote proliferative progenitor divisions in the developing mouse cerebral cortex. Development 2008;135:11–22.

8   Siegenthaler JA, Ashique AM, Zarbalis K et al. Retinoic acid from the meninges regulates cortical neuron generation. Cell 2009;139:597–609.

9   Doetsch F, Caillé I, Lim DA et al. Subventricular zone astrocytes are neural stem cells in the adult mammalian brain. Cell 1999;97:703–716.

10 Gregg C, Weiss S. CNTF/LIF/gp130 receptor complex signaling maintains a VZ precursor differentiation gradient in the developing ventral forebrain. Development 2005;132:565–578.

11 Sawamoto K, Wichterle H, Gonzalez-Perez O et al. New neurons follow the flow of cerebrospinal fluid in the adult brain. Science 2006;311:629–632.

12 Bartke A, Chandrashekar V, Dominici F et al. Insulin-like growth factor 1 (IGF-1) and aging: Controversies and new insights. Biogerontology 2003;4:1–8.

13 Chen RL, Kassem NA, Sadeghi M et al. Insulin-like growth factor-II uptake into choroid plexus and brain of young and old sheep. J Gerontol A Biol Sci Med Sci 2008;63:141–148.

14 Kelijman M. Age-related alterations of the growth hormone/insulin-like-growth-factor I axis. J Am Geriatr Soc 1991;39:295–307.

15 Li Y, Geng YJ. A potential role for insulin-like growth factor signaling in induction of pluripotent stem cell formation. Growth Horm IGF Res 2010;20:391–398.

16 Rafalski VA, Brunet A. Energy metabolism in adult neural stem cell fate. Prog Neurobiol 2011;93:182–203.

17 Erickson RI, Paucar AA, Jackson RL et al. Roles of insulin and transferrin in neural progenitor survival and proliferation. J Neurosci Res 2008;86:1884–1894.

18 Yamaguchi Y, Flier JS, Benecke H et al. Ligand-binding properties of the two isoforms of the human insulin receptor. Endocrinology 1993;132:1132–1138.

19 Jones JI, Clemmons DR. Insulin-like growth factors and their binding proteins: Biological actions. Endocr Rev 1995;16:3–34.

20 Denley A, Bonython ER, Booker GW et al. Structural determinants for high-affinity binding of insulin-like growth factor II to insulin receptor (IR)-A, the exon 11 minus isoform of the IR. Mol Endocrinol 2004;18:2502–2512.

21 Alagappan D, Lazzarino DA, Felling RJ et al. Brain injury expands the numbers of neural stem cells and progenitors in the SVZ by enhancing their responsiveness to EGF. ASN Neuro 2009;1:e00009.

22 Lefkovits I, Waldmann H. Limiting Dilution Analysis of Cells of the Immune System, 2nd ed. Oxford England; New York: Oxford University Press, 1999. xvi, 285.

23 Felling RJ, Snyder MJ, Romanko MJ et al. Neural stem/progenitor cells participate in the regenerative response to perinatal hypoxia/ischemia. J Neurosci 2006;26:4359–4369.

24 Levison S, McCarthy K. ''Astroglia in culture,'' Culturing Nerve Cells. In Banker G, Goslin K, eds. Cambridge: MIT Press, 1991:309–336.

25 Trenkner E. ''Cerebellar cells in culture,'' Culturing Nerve Cells. In Banker G, Goslin K, eds. Cambridge, Mass.: MIT Press, 1991:284–307.

26 Rowzee AM, Ludwig DL, Wood TL. Insulin-like growth factor type 1 receptor and insulin receptor isoform expression and signaling in mammary epithelial cells. Endocrinology 2009;150:3611–3619.

27 Furue M, Okamoto T, Hayashi Y et al. Leukemia inhibitory factor as an anti-apoptotic mitogen for pluripotent mouse embryonic stem cells in a serum-free medium without feeder cells. In Vitro Cell Dev Biol Anim 2005;41:19–28.

28 Pandini G, Frasca F, Mineo R et al. Insulin/insulin-like growth factor I hybrid receptors have different biological characteristics depending on the insulin receptor isoform involved. J Biol Chem 2002;277:39684–39695.

29 Bull ND, Bartlett PF. The adult mouse hippocampal progenitor is neurogenic but not a stem cell. J Neurosci 2005;25:10815–10821.

30 Stylianopoulou F, Efstratiadis A, Herbert J et al. Pattern of the insulin-like growth factor II gene expression during rat embryogenesis. Development 1988;103:497–506.

31 Burtrum D, Zhu Z, Lu D et al. A fully human monoclonal antibody to the insulin-like growth factor I receptor blocks ligand-dependent signaling and inhibits human tumor growth in vivo. Cancer Res 2003;63:8912–8921.

32 Novosyadlyy R, Vijayakumar A, Lann D et al. Physical and functional interaction between polyoma virus middle T antigen and insulin and IGF-I receptors is required for oncogene activation and tumour initiation. Oncogene 2009;28:3477–3486.

33 Pimentel B, de la Rosa EJ, de Pablo F. Insulin acts as an embryonic growth factor for Drosophila neural cells. Biochem Biophys Res Commun 1996;226:855–861.

34 LaFever L, Drummond-Barbosa D. Direct control of germline stem cell division and cyst growth by neural insulin in Drosophila. Science 2005;309:1071–1073.

35 Hsu HJ, Drummond-Barbosa D. Insulin levels control female germline stem cell maintenance via the niche in Drosophila. Proc Natl Acad Sci USA 2009;106:1117–1121.

36 Toyoshima Y, Monson C, Duan C et al. The role of insulin receptor signaling in zebrafish embryogenesis. Endocrinology 2008;149:5996–6005.

37 Fuss B, Becker T, Zinke I et al. The cytohesin Steppke is essential for insulin signalling in Drosophila. Nature 2006;444:945–948.

38 Pandini G, Medico E, Conte E et al. Differential gene expression induced by insulin and insulin-like growth factor-II through the insulin receptor isoform A. J Biol Chem 2003;278:42178–42189.

39 Sacco A, Morcavallo A, Pandini G et al. Differential signaling activation by insulin and insulin-like growth factors I and II upon binding to insulin receptor isoform A. Endocrinology 2009;150:3594–3602.

40 Bartlett WP, Li XS, Williams M. Expression of IGF-1 mRNA in the murine subventricular zone during postnatal development. Brain Res Mol Brain Res 1992;12:285–291.

41 Lehtinen MK, Zappaterra MW, Chen X et al. The cerebrospinal fluid provides a proliferative niche for neural progenitor cells. Neuron 2011;69:893–905.

42 Chen DY, Stern SA, Garcia-Osta A et al. A critical role for IGF-II in memory consolidation and enhancement. Nature 2011;469:491–497.

43 Bendall SC, Stewart MH, Menendez P et al. IGF and FGF cooperatively establish the regulatory stem cell niche of pluripotent human cells in vitro. Nature 2007;448:1015–1021.

44 Montes R, Ligero G, Sanchez L et al. Feeder-free maintenance of hESCs in mesenchymal stem cell-conditioned media: Distinct requirements for TGF-beta and IGF-II. Cell Res 2009;19:698–709.

45 Burns JL, Hassan AB. Cell survival and proliferation are modified by insulin-like growth factor 2 between days 9 and 10 of mouse gestation. Development 2001;128:3819–3830.

46 DeChiara TM, Efstratiadis A, Robertson EJ. A growth-deficiency phenotype in heterozygous mice carrying an insulin-like growth factor II gene disrupted by targeting. Nature 1990;345:78–80.

47 Liu JP, Baker J, Perkins AS et al. Mice carrying null mutations of the genes encoding insulin-like growth factor I (Igf-1) and type 1 IGF receptor (Igf1r). Cell 1993;75:59–72.

48 Baker J, Liu JP, Robertson EJ et al. Role of insulin-like growth factors in embryonic and postnatal growth. Cell 1993;75:73–82.

49 Louvi A, Accili D, Efstratiadis A. Growth-promoting interaction of IGF-II with the insulin receptor during mouse embryonic development. Dev Biol 1997;189:33–48.

50 Ziegler AN, Rowzee AM, Tyler WA, Wood TL and Levison SW. (2009) Distinct actions of IGF system components on murine neural stem/progenitors. *Abstracts, SfN meeting*, Washington, DC.

See www.StemCells.com for supporting information available online.